TITLE: Adaptation and coordinated evolution of plant hydraulic traits.

Pablo Sanchez-Martinez, Jordi Martínez-Vilalta, Kyle G. Dexter, Ricardo A. Segovia and Maurizio Mencuccini

Affiliations and emails:

Pablo Sanchez-Martinez[1,2]: Email: p.sanchez@creaf.uab.cat Affiliations: (1) CREAF,Cerdanyola del Valles, 08193 Barcelona, Spain; (2) Universitat Autònoma de Barcelona, Cerdanyola del Valles, 08193 Barcelona, Spain

Jordi Martínez-Vilalta[1,2]: Email: Jordi.Martinez.Vilalta@uab.cat Affiliations: (1) CREAF, Cerdanyola del Valles, 08193 Barcelona, Spain (2) Universitat Autònoma de Barcelona, Cerdanyola del Valles, 08193 Barcelona, Spain

Kyle G. Dexter[3,4]: Email: Kyle.Dexter@ed.ac.uk Affiliations: (3) School of GeoSciences, University of Edinburgh, Edinburgh, United Kingdom (4) Royal Botanic Garden Edinburgh, Edinburgh, United Kingdom

Ricardo A. Segovia[3,5]: Email: segovia@ug.uchile.cl Affiliations: (3) School of GeoSciences, University of Edinburgh, Edinburgh, United Kingdom (5) Instituto de Ecología y Biodiversidad (www.ieb chile.cl), Santiago, Chile

Maurizio Mencuccini[1,6]: Email: m.mencuccini@creaf.uab.cat Affiliations: (1) CREAF, Cerdanyola del Valles, 08193 Barcelona, Spain (6) ICREA, Pg. Lluís Companys 23, 08010, Barcelona, Spain

Running title: **hydraulic traits evolution**

Keywords: global, plant hydraulics, evolution, phylogenetic comparative methods, phylogenetic mixed models, adaptation, phylogenetic conservatism, evolutionary correlation.

Type of Article: Letters

Number of words in the abstract: 150

Number of words in the main text: 5145

Number of references: 70

Number of figures: 5

Number of tables: 1

Corresponding Author: Pablo Sanchez-Martinez: p.sanchez@creaf.uab.cat, Carrer Sant Martí de Porres 1-3, 2-4, 08032 Barcelona, Spain. Telephone: +34 644376756. ORCID ID: https://orcid.org/0000-0002-0157-7800.

Author contributions: PSM, MM and JMV designed the study, KGD and RSC provided the phylogeny, JMV and MM provided the hydraulics database, PSM analysed data, with input from MM, JMV and KGD, and wrote the first draft of the manuscript. All authors contributed substantially to revisions.

Data accessibility statement: if accepted, data will be deposited in a public repository.

Abstract

Hydraulic properties control plant responses to climate and are likely to be under strong selective pressure, but their macro-evolutionary history remains poorly characterized. To fill this gap, we compiled a global dataset of hydraulic traits describing xylem conductivity (K_s), xylem resistance to embolism (P50), sapwood allocation relative to leaf area (Hv) and drought exposure (ψ_{min}), and matched it with global seed plant phylogenies. Individually, these traits present medium to high levels of phylogenetic signal, partly related to environmental selective pressures shaping lineage evolution. Most of these traits evolved independently of each other, being co-selected by the same environmental pressures. However, the evolutionary correlations between P50 and ψ_{min} and between K_s and Hv show signs of deeper evolutionary integration because of functional, developmental or genetic constraints, conforming to evolutionary modules. We do not detect evolutionary integration between conductivity and resistance to embolism, rejecting a hardwired trade-off for this pair of traits.

Introduction

Water transport in plants occurs under negative pressure and is driven by the process of transpiration at the leaf-atmosphere interface, which generates a water potential gradient throughout the plant (cohesion-tension theory) (Dixon 1914). A key source of vulnerability for the water transport system is the formation of xylem embolism, resulting from the breakage of the water columns caused by cavitation (the phase change from liquid water to gas), which reduces hydraulic conductivity and may lead to plant death through hydraulic failure (Tyree & Zimmermann 2002). This process is more likely to occur during drought events, as low water availability results in low soil plant water potentials, and becomes more pronounced also with high temperatures, which provoke an increase in atmospheric evaporative demand (Venturas *et al.* 2017). A wealth of research over the last decades has established that hydraulic failure is a principal mechanism triggering tree mortality under drought (Adams *et al.* 2017). Therefore, drought and high temperatures, together with other important sources of selection such as freezing temperatures (Zanne *et al.* 2014), have been considered among the primary forces shaping plant evolution by acting directly on hydraulic traits (Maherali *et al.* 2004). However, global patterns in the evolution of hydraulic traits remain only partly characterized and their relationship with relevant environmental selective pressures poorly identified.

Species differ greatly in their exposure to low water potentials and in their capacity to operate under such conditions. The actual hydraulic risk is normally represented by the hydraulic safety margin (HSM) (Choat *et al.* 2012). HSM integrates both drought stress exposure at the tissue level, measured as the minimum leaf water potential registered for a given species (ψ_{min}), and resistance to embolism, quantified as the water potential that causes a 50% reduction in stem hydraulic conductivity (P50) (HSM = ψ_{min} - P50). Plants with low (or even negative) safety margins

experience large amounts of embolism (Choat *et al.* 2012, 2018). ψ_{min} emerges from the balance between soil water availability, the rate of water loss, and the capacity of the plant transport system to supply water to leaves, and it is thus determined by plant functional properties such as rooting strategy, leaf phenology and stomatal control as well as by abiotic factors such as soil water availability and atmospheric evaporative demand (Bhaskar & Ackerly 2006). Meanwhile, P50 is primarily explained by xylem anatomical features (Venturas *et al.* 2017). P50 and ψ_{min} are known to co-vary, leading to relatively invariant HSMs at the global scale and to respond to similar environmental selective pressures related to water availability (Choat *et al.* 2012). For instance, stem P50 has been reported to be negatively related with precipitation for 10 conifer species from different habitats (Brodribb & Hill 1999) and for the gymnosperm genus *Callitris* (Larter *et al.* 2017) and ψ_{min} has been positively related to variables determining water availability (Bhaskar & Ackerly 2006) and negatively to soil particle size during drought for Great Basin shrubs (Sperry & Hacke 2002). Since the risk of hydraulic failure is likely to be under greater selective pressure than ψ_{min} and P50 *per se*, these two latter traits are expected to be integrated over the evolutionary history of lineages, specifically meaning that they evolve in a coordinated fashion (i.e., non-independently from each other), representing an evolutionary module.

Xylem conductive capacity is another key determinant of hydraulic function, usually quantified as the maximum, stem-specific hydraulic conductivity (K_s). This property has been reported to be positively related to temperature and precipitation at a global scale (He *et al.* 2020). Because the structural properties of xylem conduits and pit membranes associated with increased embolism resistance (quantified here as P50) are also expected to reduce conductive capacity, a trade-off between P50 and K_s has long been hypothesized (often referred to as the hydraulic safety-efficiency trade-off) (Tyree & Zimmermann 2002). According to this hypothesis, evolutionary

processes associated with frequent drought occurrence would have driven an increase of xylem resistance to embolism, allowing taxa to bear lower water potentials and maintain water transport at the expense of xylem conductive capacity. In contrast, increased xylem conductivity could have evolved in wetter and warmer environments, where higher water transport was adaptive and selective pressures favouring expensive safety features were weaker (Maherali *et al.* 2004). Although this trade-off has been shown to be relatively weak across species (e.g. Maherali *et al.* 2004; Gleason *et al.* 2016), it remains unknown whether it reflects independent responses of each trait to similar selective pressures related to climate conditions and soil properties, or a deeper evolutionary integration.

The role of hydraulic conductivity is more nuanced when considered at the whole plant level, where transport capacity needs to match water demand, which is in turn strongly influenced by leaf area (Mencuccini *et al.* 2019b). Consequently, xylem conductive capacity is frequently expressed in a relativized manner as a measure of hydraulic sufficiency (leaf-specific hydraulic conductivity; K_l, $K_l = K_s$ * Hv, see below) (Tyree & Zimmermann 2002). From this perspective, plants may adapt to drought stress prioritizing supply over demand by reducing the ratio of leaf area relative to cross-sectional sapwood area (i.e., increasing its inverse, the Huber value; Hv) and thus ensuring the maintenance of hydraulic sufficiency under water scarcity. Contrarily, lineages not exposed to drought stress and with no restriction to evolve towards a more conductive xylem may be able to supply water to a higher leaf area by using a relatively low sapwood area, potentially allowing for higher productivity (Mencuccini *et al.* 2019b). Therefore, we would also expect xylem conductivity and sapwood-to-leaf allocation to be integrated over evolutionary timescales, evolving in a coordinated manner to maintain hydraulic sufficiency (Reich *et al.* 2003).

In this study, we aim to elucidate the global macro-evolutionary patterns of hydraulic traits, disentangling (1) the degree to which trait values are evolutionarily conserved along the phylogeny, (2) the extent to which trait conservatism is related to environmentally driven selection and (3) whether traits evolve in a correlated manner because of their independent responses to similar environmental conditions or because of a deeper integration, in which case they may represent evolutionary modules (i.e., a set of traits that co-evolve). We hypothesize that closely related species will have more similar trait values than expected by chance (Losos 2008) and that phylogenetic conservatism will be partly explained by environmental selection (Fig. 1). In addition, we hypothesize that some pairs of traits will show signs of a direct evolutionary relationship (evolutionary modules) reflecting a deep functional, developmental or genetic integration. Specifically, we expect to find three evolutionary modules consistent with previously hypothesized trait coordinations (namely, P50/ψ_{min}, P50/K_s, K_s/Hv).

Materials and methods

Data sources

We extracted detailed hydraulic trait data from a database covering 2027 species (1888 angiosperms and 139 gymnosperms), representing 817 genera from 161 families. Most of the data come from a previously published database (Mencuccini *et al.* 2019b), which was supplemented with the database reported by Liu *et al*. (2019). Species names were matched against accepted names in The Plant List using the "taxonstand" R package (Cayuela *et al.* 2012). Then, the "taxonlookup" R package (Pennell *et al.* 2016) was used to complete species information at the genus, family, order and major evolutionary affiliation (angiosperms vs. gymnosperms) levels. The database covers all major biomes (Fig. S1 in Supporting Information).

We used data of four hydraulic traits that were represented across sufficiently large numbers of

species (N > 550): (1) maximum stem-specific hydraulic conductivity (K_s, kg m^{-1} MPa^{-1} s^{-1}) as a measure of xylem conductive capacity; (2) stem water potential at 50% loss of hydraulic conductivity measured in terminal branches (P50, MPa) as a measure of xylem resistance to embolism; (3) branch-based Huber value (Hv; cm^2 m^{-2}), defined as the sapwood cross-sectional area to leaf area ratio, as a measure of allocation; and (4) minimum midday leaf water potential recorded for species (ψ_{min}, MPa) as a measure of exposure to drought stress at the tissue level. We also included two additional variables integrating two pairs of the four selected traits, specifically, (5) maximum leaf-specific hydraulic conductivity (K_l, kg m^{-1} MPa^{-1} s^{-1}) as the hydraulic capacity per unit leaf area (K_s * Hv) and (6) the hydraulic safety margin (HSM, HSM = ψ_{min} – P50) (Table S1). When multiple measures for one species were available, mean values were used for all traits, except for ψ_{min}, where the absolute minimum was used (c.f. Choat *et al.* 2012). For all variables, we excluded data from seedlings and studies in greenhouses or experimental gardens, data obtained on roots and leaves (Liu *et al.* 2019; Mencuccini *et al.* 2019b) and P50 values corresponding to extreme, r-shaped vulnerability curves, following the same criteria as in Choat *et al.* (2012).

We note that all study traits are subject to methodological uncertainty in their determination and in aggregation to species level, and sample sizes differ among species. Estimates of species-specific ψ_{min} in particular are sample-size dependent and likely biased to an unknown extent for some species. It is likely that the sampling period will miss droughts with a long return interval at some sites. It is also likely that long-lived species (e.g. several gymnosperms) will encounter more severe drought events throughout their lives with consequently greater biases. HSM combines uncertainties in both P50 and ψ_{min} determination, which is problematic because of direct methodological issues in the case of P50 (Jansen *et al.* 2015) and because of the inherent difficulty

in characterizing extreme values in the case of ψ_{min} (Head *et al.* 2012). Finally, in the case of K_s, although it is normalized by sapwood area, it might still depend upon stem size to some degree.

Sixteen environmental variables were compiled (11 related to climate and five to soil properties) (Table S1). Climatic variables were extracted from WorldClim (Fick & Hijmans 2017) (www.worldclim.org; accessed on February 2019) except for Moisture Index, which was extracted from the global aridity and potential evapotranspiration (PET) database (Trabucco & Zomer 2019) (http://www.cgiar-csi.org, data accessed on February 2019) at a resolution of 30 arcsec. Soil data were extracted from SoilGrids (Hengl *et al.* 2017) (https://soilgrids.org/, accessed on February 2019) at the same resolution. Occurrences for all species were obtained from the Global Biodiversity Information Facility (https://www.gbif.org/es/ accessed on February 2019) and the Atlas of Living Australia (http://www.ala.org.au. accessed on February 2019) using the "rgbif" (Chamberlain *et al*. 2020) and the "ALA4R" (Raymond, Vanderwal & Belbin 2014) R packages, respectively. Potentially incorrect species occurrence records where filtered using the "CoordinateCleaner" R package (Zizka *et al.* 2019).

Phylogeny

We used a genus-level phylogeny instead of a species-level one to avoid issues with species misidentifications, which are particularly common in the tropics (Baker *et al.* 2017), and from where a considerable amount of our hydraulics data come. The genera in the phylogeny covered a greater number of species present in our database than the best-sampled species-level phylogeny available (Smith & Brown 2018). Some models, however, were also fitted using the species-level phylogeny from Smith & Brown (2018), to assess the robustness of our results to the taxonomic resolution of our phylogenetic data. To construct the genus-level phylogeny, sequences of the *rbc*L and *mat*K plastid gene for 707 angiosperm tree genera were obtained from Genbank

(www.ncbi.nlm.nih.gov/genbank/) building on previous efforts (Dexter & Chave 2016; Neves *et al.* 2020; Segovia et al. 2020). Sequences were aligned using the MAFFT software (Katoh & Standley 2013). "Ragged ends" of sequences that were missing data for most genera were manually deleted from the alignment. The two chloroplast markers were concatenated, and a maximum likelihood phylogeny for the genera was estimated in the RAxML v8.0.0 software (Stamatakis *et al.* 2008), on the CIPRES web server (www.phylo.org), using General Time Reversible (GTR) + categorical Gamma (G) model of sequence evolution. The tree was constrained following order-level relationships proposed by the angiosperm Phylogeny Group IV (Chase *et al.* 2016). Sequences of *Nymphaea alba* (Nymphaeaceae) were included as an outgroup.

The resulting maximum likelihood phylogeny for angiosperms was temporally calibrated using the software treePL (Smith & O'Meara 2012). Age constraints for internal nodes were implemented for most families and orders (Magallón *et al.* 2015). The rate smoothing parameter (lambda) was set to 10 based on a cross-validation procedure. Finally, the newly-derived angiosperm phylogeny was fused with an existing gymnosperm phylogeny (Leslie *et al.* 2018). We manually added the genera *Gnetum* and *Ginkgo* according to ages found in the literature, 174 Ma for the Gnetales (Ran *et al.* 2018) and 265.2 Ma for Ginkgoaceae (Tank *et al.* 2015).

Statistical analyses

All analyses were carried out in R (3.6.0) (R Core team 2019). Some variables were transformed to achieve normality (using absolute values in the case of P50 and ψ_{min}) (Table S1). A Principal Components Analysis (PCA) on the 16 variables was performed using the R package "stats" (R Core team 2019) to reduce the number of axes summarizing environmental variation. The first principal component (PC1) explained 51% of the variance in the environmental data, representing variation in water availability and some related variables such as soil pH, soil clay content, soil

water content and temperature seasonality, with high values characterizing more humid locations with leached acidic soils characteristic of non-seasonal wet tropical habitats. The second principal component (PC2) explained 20% of the variance, representing variation in energy input, with high values characterizing low solar irradiation, low maximum temperatures and low atmospheric water demand. Finally, the third principal component accounted for 9% of the variance and largely reflected soil depth and, to a lower extent, wind velocity, with high values indicating deeper soils with low sand content and low maximum wind velocities (Table S2, Fig. S2 and Fig. S3). The remaining components explained a low proportion of variance (<7%), so the first three axes were used to characterize the environmental niches of species in the following analyses.

Uni-response and bi-response Bayesian phylogenetic mixed models, alternatively including or excluding fixed effects of environmental principal components, major evolutionary affiliation (angiosperm vs. gymnosperm) and their interactions were fitted using the "MCMCglmm" R package (Hadfield 2010) (see Table S3 for models description). All models accounted for the occurrence of multiple measurements in each genus by the inclusion of genus identity as a random effect. Moreover, genus-level phylogenetic relationships were taken into account as a second random effect using the previously presented phylogeny. The inclusion of these random effects allowed us to partition the residual variance from models into three components: the inter-generic variance caused by phylogenetic relationships; the non-phylogenetic, inter-generic variance; and the intra-generic variance. The inter-generic phylogenetic variance quantifies the variability explained by the relationships among taxa as given by our phylogenetic hypothesis and, when divided by the total variance, gives a measure of the phylogenetic signal (λ) (Lynch 1991). Non-phylogenetic inter-generic variance (γ) accounts for the proportion of among-genus variability not explained by the phylogeny, and the intra-generic variance (ρ) provides a measure of the

proportion of variability caused by intra-generic trait variation (plus any residual error) (Hadfield & Nakagawa 2010) (see Appendix S1 for a more formal description).

To partition variances of phylogenetic and non-phylogenetic components, we implemented uni-response models without fixed effects for the six selected hydraulic traits and for the three environmental PCA axes as response variables (Table 1, Table S4 to see non-phylogenetic model variance partitions). To identify relationships between hydraulic traits and environmental PCA axes, we then ran uni-response models with hydraulic traits as response variables and single environmental principal components as fixed effects, both accounting and not accounting for phylogenetic relationships affecting the response trait. To examine the effect of the major split between angiosperms and gymnosperms, additional models included a binary variable describing major evolutionary affiliation and the interaction between affiliation and environment, allowing us to detect statistical differences between angiosperms and gymnosperms in the overall mean values of traits and in their relationships with environmental axes. For each group of nested models, the best fitting one in terms of DIC (Deviance Information Criterion) was selected (Table S5 to see DIC values). Models within 4 DIC units of each other were considered equivalent in terms of fit, and the simplest one was selected.

Subsequently, to characterize phylogenetic covariation between the hydraulic traits and between each hydraulic variable and the three environmental principal components, bi-response models were used. In these models, two response variables and their phylogenetic structure were considered simultaneously, resulting in a variance-covariance matrix from which the evolutionary correlation between the two variables could be calculated (Appendix S1). Evolutionary correlations were calculated for all combinations of trait pairs, including and excluding the three environmental components, evolutionary affiliation and their interactions as fixed effects (Fig. S1

shows data coverage for each combination of traits). Finally, we also estimated evolutionary correlations between traits and single environmental principal components including and excluding evolutionary affiliation as a fixed effect (Table S6 to see all correlations). Bi-response models were also implemented using the species-level phylogeny reported by Smith & Brown (2018) and available in the R package "v.PhyloMaker" (Jin & Qian 2019), to ensure consistency with genus-level results (see Apendix S2). As data availability for the species-level phylogeny was lower, we replicated the bi-response genus-level models using the same reduced dataset to ensure that potential differences between results were not due to different species coverage. We also performed analyses using the species-level phylogeny pruned at the genus-level, to ensure that potential differences between results were not explained by differences in the topologies of our custom-made genus-level phylogeny and the available species-level phylogeny (Appendix S3).

Models were specified to achieve convergence while minimizing correlation between iterations (Appendix S1). Marginal variance explained (R^2_m, variance explained by the fixed effects) and conditional variance explained (R^2_c, variance explained by both fixed and random effects) were calculated for the uni-response models (Nakagawa & Schielzeth 2013). P-values were calculated for evolutionary correlations following Makowski *et al*. (2019).

Finally, reconstructions of the six traits and the three environmental principal components evolution under a Brownian motion model were mapped along the phylogeny using maximum likelihood ancestral state reconstructions (Schluter *et al.* 1997) by means of the "Phytools" R package (Revell 2013).

Results

Phylogenetic and non-phylogenetic variances

All six selected traits showed a significant phylogenetic signal. The proportion of variance that was explained by the inter-generic phylogenetic structure (λ) ranged from 0.432 (K_l) to 0.745 (ψ_{min}) (Table 1). This means that 43.2-74.5% of trait variances can be attributed to relatively deep evolutionary differences among genera, with the rest being attributed to non-phylogenetically correlated inter-generic (γ) and intra-generic (ρ) variances. Intra-generic variances (ρ) ranged from 0.189 (ψ_{min}) to 0.532 (K_l), being the second most important variance component in all cases except K_l (where it was the most important), indicating that trait diversification within genera is a substantial generator of global trait variability. Analyses using the species-level phylogeny confirmed that variation within genera also had strong phylogenetic patterns (Appendix S2). Finally, inter-generic, non-phylogenetically related variances (γ) ranged from 0.036 (K_l) to 0.225 (P50) and accounted for the lowest proportion of the variance in all cases (Table 1). Phylogenetic mapping of hydraulic traits qualitatively confirmed the findings reported above, showing more gradual changes in highly conserved traits such as ψ_{min} and changes more concentrated at the tips of the phylogeny for variables showing a lower phylogenetic signal, such as Hv, which also showed higher intra-generic variance (Fig. 2, Fig. 3 and Fig. S4).

Importantly, the phylogenetic signal of the three environmental principal components was also very high, particularly for PC1, representing water availability (0.820) and PC3, mainly represented by soil depth (0.841) (Table 1, Fig. S5).

Environmental drivers of hydraulic trait variability

In models that accounted for phylogenetic structure, all hydraulic traits showed significant relationships with at least one of the three environmental axes defined by the PCA (Fig. 4).

Conditional explained variances (R^2_c) were notably higher than marginal explained variances (R^2_m), indicating that accounting for the phylogenetic relationships was crucial to improve model fit (Fig. 4). Consistent with the fact that environmental axes were highly phylogenetically conserved, we also found that the phylogenetic signal of traits (Table 1) diminished when accounting for environmental effects (Fig. 4, lambdas (λ)), thus indicating that environmental conditions explain part of the phylogenetic variance.

Xylem resistance to embolism (|P50|) was only negatively related to PC1 (water availability). Minimum water potential at midday ($|\psi_{min}|$) was negatively related to PC1 and PC2 (declining energy input) and positively to PC3 (soil depth). However, the relationship with PC1 was only significant for angiosperms. Xylem conductivity (K_s) was found to be positively related to PC1 and PC3, being negatively related with PC2 only in non-phylogenetic models. Sapwood to leaf area ratio (Hv) was negatively related to PC1 and PC3. The hydraulic safety margin (HSM) was positively related to PC1 and PC2 only for angiosperms and the relationship between HSM and PC3 was only significant (and negative) for non-phylogenetic models. Finally, Leaf-specific conductivity (K_l) was only related to PC2 (negatively) in phylogenetic models, but a positive relationship with PC3 was also found when using non-phylogenetic models (Fig. 4).

Evolutionary correlations

Significant evolutionary correlations were reported between $|\psi_{min}|$ and |P50| (positive), K_s and Hv (negative), Hv and |P50| (positive) (Fig. 5). These evolutionary correlations were confirmed when the species-level phylogeny was used, which also showed a significant evolutionary correlations between |P50| and K_s (negative), $|\psi_{min}|$ and Hv (positive) and K_s and $|\psi_{min}|$ (negative) (Fig. S6). The emergence of these evolutionary correlations was not explained by the lower number of species available for the species-level phylogeny compared to the genus-level one, nor by differences in

topology between phylogenies (Appendix S3), so it is likely due to the large amount of phylogenetic covariance between traits within genera. Only two evolutionary correlations between traits remained once environmental factors and major evolutionary affiliation of species were accounted for, coinciding with two of the three hypothesized evolutionary modules. These were the ones involving |P50| and $|\psi_{min}|$ (positive correlation) and K_s and Hv (negative correlation) (Fig. 5, Fig. S6). While |P50| and $|\psi_{min}|$ presented a highly conserved covariation pattern, the evolutionary integration between K_s and Hv was less strong. The latter was marginally significant when using the genus-level phylogeny (Fig. 5), but clearly significant when intra-generic phylogenetic covariation between traits was additionally considered by using the species-level phylogeny (Fig, S6).

Consistent evolutionary correlations were also observed between certain hydraulic traits and environmental principal components in the bi-response models: K_s was positively correlated with PC1 (water availability), and PC3 (soil depth) while its relationship with PC2 (energy input) was only significant at the genus-level and disappeared when considering major evolutionary affiliation. Hv was negatively correlated with PC1 and PC3; and both |P50| and $|\psi_{min}|$ were negatively correlated with PC1 (Fig. 5).

Discussion

Conservatism and adaptation in hydraulic trait evolution

We found a clear pattern of phylogenetic conservatism for hydraulic traits, suggesting that the legacy of traits found in species' evolutionary ancestors is an important determinant of trait values in extant species. While we cannot formally rule out Brownian motion evolution operating over long evolutionary timescales as the source of present-day trait variability on the basis of our single trait variance partitioning (Revell *et al*. 2008), our finding of evolutionary correlations of traits

with environmental variables indicates a key role for non-random evolutionary processes. Moreover, environmental components explained part of traits' phylogenetic variance when accounted for as fixed effects (Fig. 4). Therefore, our analyses indicate that adaptive processes have driven the diversification of hydraulic traits, but the prevalent pattern of phylogenetic niche conservatism suggests that evolutionary constraints have limited the range of trait values within lineages. Thus, lineages have been largely tracking environments similar to those their ancestors were already adapted to, retaining ancestral traits because of stabilizing selection (Ackerly 2009), while occasionally adapting to novel environmental conditions.

We do observe a wide range of trait values across lineages (including among genera), indicating that they adaptively diverged in deep evolutionary time (Fig. 2, Fig. 3, Fig. S4 and Fig. S5). Further, substantial trait variation can also arise over shorter evolutionary timescales (i.e., in recent evolutionary time) via species adapting to present-day selective pressures, as supported by the significant degree of trait variance at the intra-generic level (Table 1), which also appears to have a phylogenetic component (Fig. S6, Appendix 2). As a result, lineages that have been evolving in dry habitats have adapted to a higher exposure to drought stress by increasing their xylem resistance to embolism, being able to maintain water transport at low water potentials (Choat *et al.* 2012). These species are also selected to ensure water supply to leaves by using a relatively high sapwood area with a low hydraulic conductivity (Mencuccini *et al.* 2019b). As water become less limiting, lineages are less exposed to low water potentials and are not selected to increase xylem resistance to embolism, while switching their allocation priority to a high leaf area maintained by a smaller area of highly conductive sapwood (Fig. 4).

However, substantial variability in species exposure to drought stress within a given environment reflects the fact that plant characteristics such as stomatal control (Brodribb & McAdam 2017),

deciduousness (Wolfe *et al.* 2016) or rooting depth (Canadell *et al.* 1996) are also determining hydraulic trait evolution. This may explain the lack of a relationship between PC1 (water availability) and ψ_{min} and HSM in gymnosperms, a clade mainly represented by Pinaceae and Cupressaceae (Fig. S7) that are known to adopt contrasting strategies under drought. While Pinaceae avoid exposure to low water potentials by closing their stomata and possibly disconnecting from the soil (Poyatos *et al.* 2018), Cupressaceae tolerate them by presenting a high resistance to embolism (Brodribb *et al.* 2014). Differences between angiosperms and gymnosperms could also be due to an underestimation of drought stress exposure for long-lived gymnosperms, especially in the case of the highly stress-resistant Cupressaceae, for which the observation window may not have been long enough to adequately capture ψ_{min}. Therefore, different evolutionary processes may be dominant depending on the taxon studied. For instance, xylem resistance has been reported to be extremely labile for the genus *Callitris* (Larter *et al.* 2017) and to be conserved for *Juniperus* (Willson *et al*. 2008), while showing a high canalization for *Pinus* species (Lamy *et al.* 2014). It is also worth noting that our global eco-evolutionary overview may be limited by the availability of hydraulic data and its methodological uncertainties, as well as by the difficulty of upscaling traits at the whole-plant level, which remains a challenge (Mencuccini *et al.* 2019a).

Evolutionary modules in hydraulic traits

Traits can evolve in an apparently coordinated fashion because of their response to similar selective pressures, but direct relationships between them may also arise from functional, developmental or genetic constraints, conforming to evolutionary modules. We found two sets of traits for which an evolutionary correlation cannot be explained by similar, albeit independent responses to environmental conditions or by fundamental differences between angiosperms and gymnosperms.

These sets of traits represent a deeper evolutionary integration, confirming two of the three hypothesized evolutionary modules. The first evolutionary module involves species exposure to drought and resistance to embolism (P50/ψ_{min}), and it is strongly conserved over evolutionary scales. The second one involves xylem conductivity and sapwood to leaf area allocation (K_s/Hv), the integration of which appears stronger when quantified in more recent evolutionary time (c.f. results for genus- vs. species-level phylogenies in Fig. 5 and Fig. S6). The third evolutionary module we hypothesized (K_s/P50) appears to be explained exclusively by separate trait responses to similar selective pressures, confirming previous results (Maherali *et al.* 2004). Therefore, a direct evolutionary trade-off between K_s and P50 can be rejected based on available data, further indicating that K_s and P50 cannot be determined by a single common anatomical feature (e.g., the size distribution of pores in the inter-conduit pit membranes) (Baas *et al.* 2004). We suggest that K_s and P50 depend on several anatomical properties that may be coordinated under strong selective pressures, but do not necessarily co-evolve when pressures are relaxed over evolutionary timescales. Our results likely reflect the fact that some species may present strategies that do not rely on maximizing xylem conductivity or resistance to embolism, especially when water is not the most limiting resource and survival does not depend on fast resource use (Reich 2014). However, the detailed structural and physiological conditions allowing the independent evolution of these two traits remains to be elucidated.

Traits involved in the same evolutionary module are likely to be functionally, developmentally and genetically integrated. Deep functional integrations over evolutionary times can be explained by the need to optimize HSM and K_l under a given environmental context, as the maintenance of positive safety margins and a sufficient hydraulic supply to leaves are likely to be closely linked to survival (Choat *et al.* 2018) and under a strong stabilizing selection. Therefore, events of

coordinated directional selection on the involved trait pairs described above might take place over evolutionary times in order to maintain HSM and K_l values close to the adaptive peak. The conservative nature of the relationship between Hv and K_s also reflects broader strategies of convergent evolution integrating hydraulic with photosynthetic and nutrient-use traits as a function of water availability (Hao *et al.* 2011; Liu *et al.* 2015).

Integration might also be influenced by phylogenetic conservatism in underlying physiological processes and anatomical features. For example, conservatism in stomatal control (Brodribb & McAdam 2017) and leaf phenology (Davies *et al.* 2013) might explain the evolutionary covariation between ψ_{min} and P50 beyond environmental forcing, with some lineages being able to avoid low water potentials by rapid stomatal closure (Martin-StPaul *et al.* 2017) or drought-deciduousness (Kolb & Davis 1994).

Finally, these functional and developmental integrations may be underpinned by genetic integration, specifically meaning that processes such as genetic correlation (Etterson & Shaw 2001), linkage disequilibrium and pleiotropy (Cheverud 1996) might be affecting the anatomical and structural determinants of the traits involved, leading to the observed evolutionary integration. As a result, the evolution of traits in the same module might be genetically constrained (Wagner 1996). Further work on the causes and consequences of the evolutionary integration of hydraulic traits, and the meaning of their conservatism through evolutionary time, will be crucial to characterize global trait syndromes and assess species adaptive potential under changing environmental conditions.

Conclusion

Hydraulic traits are under strong selective control and appear to be largely determined by deep-time evolutionary changes driven by adaptation to divergent environmental conditions, in turn limited by evolutionary constraints. We have found evidence for evolutionary integrations not explained by common environmental drivers, conforming to two evolutionary modules: the xylem resistance-exposure module (ψ_{min}/P50), which is highly conserved over evolutionary scales, and the conductivity-allocation module (Hv/K_s), which is more evident in recent evolutionary time. Our results do not support the hypothesized resistance-conductivity module (K_s/P50). The underlying mechanisms shaping these evolutionary modules and their role in species functional and evolutionary diversification remain to be elucidated. More phylogenetically explicit studies of individual clades (including intraspecific genetic, anatomical and functional variation) under different environmental contexts will allow further characterization of plant trait syndromes as a network of integrated units that respond to natural selection.

Acknowledgments

This work was supported by the Spanish government via competitive grants FUN2FUN (CGL2013-46808-R) and DRESS (CGL2017-89149-C2-1-R).We would like to thank Lucy Rowland, Toby Pennington, Paulo Bittencourt and Mario Marcos do Espirito Santo, and Jarrod Hadfield in particular, for fruitful discussions and insights on previous versions of the manuscript, as well as to Brendan Choat, Steven Jansen and Hui Liu for their previous work on data compilation. P.S.-M. acknowledges an FPU predoctoral fellowship from the Spanish Ministry of Science, Innovation and Universities (grant FPU18/04945). J.M.-V. benefited from an ICREA Academia award. R.A.S. is supported by a Newton International Fellowship from The Royal Society, by Conicyt PFCHA/Postdoctorado Becas Chile/2017 N° 3140189 and by CONICYT PIA

APOYO CCTE AFB170008. The data derived from the hydraulics database are partly an outcome from a working group funded by the Australian Research Council (ARC) through the Australia-New Zealand Research Network for Vegetation Function.

Literature cited

Ackerly, D. (2009). Conservatism and diversification of plant functional traits: Evolutionary rates versus phylogenetic signal. *Proc. Natl. Acad. Sci.*, 106, 19699–19706.

Adams, H.D., Zeppel, M.J.B., Anderegg, W.R.L., Hartmann, H., Landhäusser, S.M., Tissue, D.T., *et al*. (2017). A multi-species synthesis of physiological mechanisms in drought-induced tree mortality. *Nat. Ecol. Evol.*, 1, 1285–1291.

Baas, P., Ewers, F.W., Davis, S.D. & Wheeler, E.A. (2004). Evolution of xylem physiology. In: (The evolution of plant physiology) {Hemsley, A.R., Poole, L.}. Elsevier, London, 273–295.

Baker, T. R., Pennington, R. T., Dexter, K. G., Fine, P. V. A., Fortune-Hopkins, H., Honorio, E. N., *et al*. (2017). Maximising Synergy among Tropical Plant Systematists, Ecologists, and Evolutionary Biologists. *Trends Ecol Evol.*, 32(4), 258–267.

Bhaskar, R. & Ackerly, D.D. (2006). Ecological relevance of minimum seasonal water potentials. *Physiol. Plant.*, 127, 353–359.

Brodribb, T. & Hill, R.S. (1999). The importance of xylem constraints in the distribution of conifer species. *New Phytol.*, 143, 365–372.

Brodribb, T.J. & McAdam, S.A.M. (2017). Evolution of the stomatal regulation of plant water content. *Plant Physiol.*, 174, 639–649.

Brodribb, T.J., McAdam, S.A.M., Jordan, G.J. & Martins, S.C.V. (2014). Conifer species adapt to low-rainfall climates by following one of two divergent pathways. *Proc. Natl. Acad. Sci.*, 111, 14489–14493.

Canadell, J., Jackson, R.B., Ehleringer, J.R., Mooney, H.A., Sala, O.E. & Schulze, E.D. (1996). Maximum rooting depth of vegetation types at the global scale. *Oecologia*, 108, 583–595.

Cayuela, L., Granzow-de la Cerda, Í., Albuquerque, F.S. & Golicher, D.J. (2012). Taxonstand: An r package for species names standardisation in vegetation databases. *Methods Ecol. Evol.*, 3, 1078–1083.

Chamberlain S., Barve V., Mcglinn D., Oldoni D., Desmet P., Geffert L. & Ram K. (2020). rgbif: Interface to the Global Biodiversity Information Facility API. R package version 2.2.0.

Chase, M.W., Christenhusz, M.J.M., Fay, M.F., Byng, J.W., Judd, W.S., Soltis, D.E., *et al*. (2016). An update of the Angiosperm Phylogeny Group classification for the orders and families of flowering plants: APG IV. *Bot. J. Linn. Soc.*, 181, 1–20.

Cheverud, J.M. (1996). Developmental integration and the evolution of pleiotropy. *Am. Zool.*, 36, 44–50.

Choat, B., Brodribb, T., Brodersen, C., Duursma, R., López, R. & Medlyn, B. (2018). Triggers of tree mortality under drought drought and forest mortality. *Nature*, 558, 531–539.

Choat, B., Jansen, S., Brodribb, T.J., Cochard, H., Delzon, S., Bhaskar, R., *et al*. (2012). Global convergence in the vulnerability of forests to drought. *Nature*, 491, 752–755.

Davies, T.J., Wolkovich, E.M., Kraft, N.J.B., Salamin, N., Allen, J.M., Ault, T.R., *et al*. (2013). Phylogenetic conservatism in plant phenology. *J. Ecol.*, 101, 1520–1530.

462 Dexter, K. & Chave, J. (2016). Evolutionary patterns of range size, abundance and species richness
463 in Amazonian angiosperm trees. *PeerJ*, 2016, 1–14.

464 Dixon, H.H. (1914). *Transpiration and the ascent of sap in plants.* MacMillan, London, UK.

465 Etterson, J.R. & Shaw, R.G. (2001). Constraint to adaptive evolution in response to global
466 warming. *Science*, 294, 151–154.

467 Fick, S.E. & Hijmans, R.J. (2017). WorldClim 2: new 1-km spatial resolution climate surfaces for
468 global land areas. *Int. J. Climatol.*, 37, 4302–4315.

469 Gleason, S.M., Westoby, M., Jansen, S., Choat, B., Hacke, U.G., Pratt, R.B., *et al.* (2016). Weak
470 trad eoff between xylem safety and xylem-specific hydraulic efficiency across the world's woody
471 plant species. *New Phytol.*, 209, 123–136.

472 Hadfield, J.D. (2010). MCMCglmm for R. J. *Stat. Softw.*, 33.

473 Hadfield, J.D. & Nakagawa, S. (2010). General quantitative genetic methods for comparative
474 biology: Phylogenies, taxonomies and multi-trait models for continuous and categorical
475 characters. *J. Evol. Biol.*, 23, 494–508.

476 Hao, G.Y., Goldstein, G., Sack, L., Holbrook, N.M., Liu, Z.H., Wang, A.Y., *et al*. (2011). Ecology
477 of hemiepiphytism in fig species is based on evolutionary correlation of hydraulics and carbon
478 economy. *Ecology*, 92, 2117–2130.

479 He, P., Gleason, S.M., Wright, I.J., Weng, E., Liu, H., Zhu, S., *et al*. (2020). Growing-season
480 temperature and precipitation are independent drivers of global variation in xylem hydraulic
481 conductivity. *Glob. Chang. Biol.*, 26, 1833–1841.

Head, A.W., Hardin, J.S. & Adolph, S.C. (2012). Methods for estimating peak physiological performance and correlating performance measures. *Environ. Ecol. Stat.*, 19, 127–137.

Hengl, T., Mendes de Jesus, J., Heuvelink, G. B. M., Ruiperez Gonzalez, M., Kilibarda, M., Blagotić, A., *et al*. (2017). SoilGrids250m: Global gridded soil information based on machine learning. *PloS One*, 12(2), e0169748.

Jansen, S., Schuldt, B. & Choat, B. (2015). Current controversies and challenges in applying plant hydraulic techniques. *New Phytol.*, 205, 961–964.

Jin, Y. & Qian, H. (2019). V.PhyloMaker: an R package that can generate very large phylogenies for vascular plants. *Ecography*, 42, 1353–1359.

Katoh, K. & Standley, D.M. (2013). MAFFT multiple sequence alignment software version 7: Improvements in performance and usability. *Mol. Biol. Evol.*, 30, 772–780.

Kolb, K.J. & Davis, S.D. (1994). Drought Tolerance and Xylem Embolism in Co-Occurring Species of Coastal Sage and Chaparral. *Ecology*, 75, 648–659.

Lamy, J.B., Delzon, S., Bouche, P.S., Alia, R., Vendramin, G.G., Cochard, H., *et al.* (2014). Limited genetic variability and phenotypic plasticity detected for cavitation resistance in a Mediterranean pine. *New Phytol.*, 201, 874–886.

Larter, M., Pfautsch, S., Domec, J.C., Trueba, S., Nagalingum, N. & Delzon, S. (2017). Aridity drove the evolution of extreme embolism resistance and the radiation of conifer genus Callitris. *New Phytol.*, 215, 97–112.

Leslie, A.B., Beaulieu, J., Holman, G., Campbell, C.S., Mei, W., Raubeson, L.R., *et al*. (2018). An overview of extant conifer evolution from the perspective of the fossil record. *Am. J. Bot.*, 105, 1531–1544.

Liu, H., Gleason, S.M., Hao, G., Hua, L., He, P., Goldstein, G., *et al*. (2019). Hydraulic traits are coordinated with maximum plant height at the global scale. *Sci. Adv.*, 5, eaav1332.

Liu, H., Xu, Q., He, P., Santiago, L.S., Yang, K. & Ye, Q. (2015). Strong phylogenetic signals and phylogenetic niche conservatism in ecophysiological traits across divergent lineages of Magnoliaceae. *Sci. Rep.*, 5, 1–12.

Losos, J.B. (2008). Phylogenetic niche conservatism, phylogenetic signal and the relationship between phylogenetic relatedness and ecological similarity among species. *Ecol. Lett.*, 11, 995–1003.

Lynch, M. (1991). Methods for the analysis of comparative data in evolutionary biology. *Evolution*, 45, 1065–1079.

Magallón, S., Gómez-Acevedo, S., Sánchez-Reyes, L.L. & Hernández-Hernández, T. (2015). A metacalibrated time-tree documents the early rise of flowering plant phylogenetic diversity. *New Phytol.*, 207, 437–453.

Maherali, H., Pockman, W.T. & Jackson, R.B. (2004). Adaptive variation in the vulnerability of woody plants to xylem cavitation. *Ecology*, 85, 2184–2199.

Makowski, D., Ben-Shachar, M. & Lüdecke, D. (2019). bayestestR: Describing Effects and their Uncertainty, Existence and Significance within the Bayesian Framework. J. *Open Source Softw.*, 4, 1541.

522 Martin-StPaul, N., Delzon, S. & Cochard, H. (2017). Plant resistance to drought depends on timely
523 stomatal closure. *Ecol. Lett.*, 20, 1437–1447.

524 Mencuccini, M., Manzoni, S. & Christoffersen, B. (2019a). Modelling water fluxes in plants: from
525 tissues to biosphere. *New Phytol.*, 222, 1207-1222.

526 Mencuccini, M., Rosas, T., Rowland, L., Choat, B., Cornelissen, H., Jansen, S., *et al*. (2019b).
527 Leaf economics and plant hydraulics drive leaf : wood area ratios. *New Phytol.* 224, 1544-1556.

528 Nakagawa, S. & Schielzeth, H. (2013). A general and simple method for obtaining R2 from
529 generalized linear mixed-effects models. *Methods Ecol. Evol.*, 4, 133–142.

530 Neves, D.M., Dexter, K.G., Baker, T.R., Coelho de Souza, F., Oliveira-Filho, A.T., Queiroz, L.P.,
531 *et al*. (2020). Evolutionary diversity in tropical tree communities peaks at intermediate
532 precipitation. *Sci. Rep.*, 10, 1188.

533 Pennell, M.W., FitzJohn, R.G. & Cornwell, W.K. (2016). A simple approach for maximizing the
534 overlap of phylogenetic and comparative data. *Methods Ecol. Evol.*, 7, 751–758.

535 Poyatos, R., Aguadé, D. & Martínez-Vilalta, J. (2018). Below-ground hydraulic constraints during
536 drought-induced decline in Scots pine. *Ann. For. Sci.*, 75.

537 Ran, J.H., Shen, T.T., Wang, M.M. & Wang, X.Q. (2018). Phylogenomics resolves the deep
538 phylogeny of seed plants and indicates partial convergent or homoplastic evolution between
539 Gnetales and angiosperms. *Proc. R. Soc. B Biol. Sci.*, 285.

540 Raymond, B., Vanderwal, J., & Belbin, L., (2014). ALA4R version 1.01. Atlas of Living
541 Australia.

R Core Team (2017). R: A language and environment for statistical computing. R Foundation for Statistical Computing, Vienna, Austria.

Reich, P. B., Wright, I. J., Cavender-Bares, J., Craine, J. M., Oleksyn, J., Westoby, M., *et al*. (2003). The Evolution of Plant Functional Variation: Traits, Spectra, and Strategies. *Int. J. Plant Sci.*, 164(S3), S143–S164.

Reich, P.B. (2014). The world-wide "fast-slow" plant economics spectrum: A traits manifesto. *J. Ecol.*, 102, 275–301.

Revell, L.J. (2013). Two new graphical methods for mapping trait evolution on phylogenies. *Methods Ecol. Evol.*, 4, 754–759.

Revell, L.J., Harmon, L.J. & Collar, D.C. (2008). Phylogenetic signal, evolutionary process, and rate. *Syst. Biol.*, 57, 591–601.

Schluter, D., Price, T., Mooers, A. Ø., & Ludwig, D. (1997). Likelihood of ancestor states in adaptive radiation. *Evolution*, 51(6), 1699–1711.

Segovia, R.A., Pennington, R.T., Baker, T.R., De Souza, F.C., Neves, D.M., Davis, C.C., *et al*. (2020). Freezing and water availability structure the evolutionary diversity of trees across the Americas. *Sci. Adv.*, 6(19), eaaz5373.

Smith, S.A. & Brown, J.W. (2018). Constructing a broadly inclusive seed plant phylogeny. *Am. J. Bot.*, 105, 302–314.

Smith, S.A. & O'Meara, B.C. (2012). TreePL: Divergence time estimation using penalized likelihood for large phylogenies. *Bioinformatics*, 28, 2689–2690.

562 Sperry, J.S. & Hacke, U.G. (2002). Desert shrub water relations with respect to soil characteristics
563 and plant functional type. *Funct. Ecol.*, 16, 367–378.

564 Stamatakis, A., Hoover, P. & Rougemont, J. (2008). A rapid bootstrap algorithm for the RAxML
565 web servers. *Syst. Biol.*, 57, 758–771.

566 Tank, D.C., Eastman, J.M., Pennell, M.W., Soltis, P.S., Soltis, D.E., Hinchliff, C.E., *et al*. (2015).
567 Nested radiations and the pulse of angiosperm diversification: increased diversification rates often
568 follow whole genome duplications. *New Phytol.*, 207, 454–467.

569 Trabucco, A. & Zomer, R.. (2019). Global Aridity Index and Potential Evapotranspiration (ET0)
570 Climate Database v2.

571 Tyree M.T. & Zimmermann M.H. (2002). *Xylem Structure and the Ascent of Sap.* Springer, New
572 York.

573 Venturas, M.D., Sperry, J.S. & Hacke, U.G. (2017). Plant xylem hydraulics: What we understand,
574 current research, and future challenges. *J. Integr. Plant Biol.*, 59, 356–389.

575 Wagner, G.P. (1996). Homologues, natural kinds and the evolution of modularity. *Am. Zool.*, 36,
576 36–43.

577 Willson, C.J., Manos, P.S. & Jackson, R.B. (2008). Hydraulic traits are influenced by phylogenetic
578 history in the drought-resistant, invasive genus *Juniperus* (Cupressaceae). *Am. J. Bot.*, 95, 299–
579 314.

580 Wolfe, B.T., Sperry, J.S. & Kursar, T.A. (2016). Does leaf shedding protect stems from cavitation
581 during seasonal droughts? A test of the hydraulic fuse hypothesis. *New Phytol.*, 212, 1007–1018.

582 Zanne, A.E., Tank, D.C., Cornwell, W.K., Eastman, J.M., Smith, S.A., Fitzjohn, R.G., *et al*.
583 (2014). Three keys to the radiation of angiosperms into freezing environments. *Nature*, 506, 89–
584 92.

585 Zizka, A., Silvestro, D., Andermann, T., Azevedo, J., Duarte Ritter, C., Edler, D., *et al*. (2019).
586 CoordinateCleaner: Standardized cleaning of occurrence records from biological collection
587 databases. *Methods Ecol. Evol.*, 10, 744–751.

Tables

Table 1. Variance partitioning for six hydraulic traits and three environmental principal components related to water availability (PC1), energy input (PC2) and soil depth (PC3). Legend: N: number of species used in each case (for which both phylogenetic and hydraulic data were available), phylogenetic variance (phylogenetic signal, λ), non-phylogenetic inter-generic variance (γ) and intra-generic variance plus measurement error (ρ). Mean and lower and upper 95% credible intervals (HDP) are shown for each component.

variable	N	λ	Lower HPD	Upper HPD	γ	Lower HDP	Upper HDP	ρ	Lower HDP	Upper HDP
Log(|P50|)	868	0.484	0.305	0.697	0.225	0.085	0.360	0.291	0.205	0.368
Log($\|\psi_{min}\|$)	541	0.745	0.572	0.874	0.066	0.000	0.179	0.189	0.129	0.273
log(K_s)	1026	0.515	0.363	0.680	0.086	0.000	0.174	0.399	0.303	0.493
Log(Hv)	1271	0.446	0.291	0.594	0.191	0.097	0.294	0.363	0.276	0.449
HSM	326	0.449	0.201	0.722	0.163	0.000	0.339	0.388	0.246	0.546
Log(K_l)	827	0.432	0.244	0.592	0.036	0.000	0.113	0.532	0.399	0.675
PC1	1911	0.820	0.767	0.870	0.063	0.030	0.099	0.117	0.093	0.139
PC2	1911	0.686	0.599	0.766	0.028	0.000	0.069	0.286	0.230	0.341
PC3	1911	0.841	0.798	0.876	0.007	0.000	0.027	0.152	0.124	0.182

Figure captions

Figure 1. Hypotheses and theoretical framework. Double-headed arrows represent potential evolutionary correlation involving key hydraulic traits (xylem conductivity (K_s), xylem resistance to embolism (P50), sapwood allocation relative to leaf area (Huber value, Hv) and drought exposure (ψ_{min})). HSM refer to Hydraulic Safety Margin, which is the relationship between ψ_{min} and P50, and K_l refer to the hydraulic sufficiency, which is the relationship between K_s and Hv. Lines represent evolutionary relationships tested between pairs of traits. Blue lines represent hypothetical positive relationships between traits, and red lines hypothetical negative ones. Black curved arrows represent traits phylogenetic variance (phylogenetic signal). Each hypothesized coordination between traits is also encircled using long dashed lines and labelled accordingly.

Figure 2. Phylogenetic reconstruction of drought exposure (ψ_{min}) and embolism resistance (P50) under a Brownian motion model of evolution. Reconstructions are made log-transformed absolute values in both cases. Families with more than one genus are presented and some of the most important families are highlighted in bold. Gymnosperm families are displayed in grey and angiosperm families in black.

Figure 3. Phylogenetic reconstruction of hydraulic conductivity (K_s) and sapwood allocation relative to leaf area (Huber value, Hv). Reconstructions are made on log-transformed data in both cases. Families with more than one genus are presented and some of the most important families are highlighted in bold. Gymnosperm families are displayed in grey and angiosperm families in black.

Figure 4. Trait-environment relationships. Relationships between environmental principal components (PC1, which is related to water availability; PC2, which is related to energy input and

PC3, which is mainly related to soil depth) and hydraulic traits (log-transformed absolute values) accounting for the phylogenetic structure of the hydraulic traits. The best model for each case is displayed, showing the Spermatophyte level relationship (black) or the angiosperm and gymnosperm relationships (red and blue, respectively) when statistically different. Grey dashed lines represent the regression line at the Spermatophyte level without accounting for the phylogenetic structure. Statistically significant ($p < 0.05$) regression slopes are displayed in bold following the same colour code. Signif. codes: '***': $P < 0.001$; '**': $P < 0.01$; '*': $P < 0.05$ '.': $P < 0.1$ ' ': $P > 0.1$. Residual phylogenetic signal (λ) once environmental effects are accounted for in each case is reported when relationships are significant. R^2_m is the variance explained by the fixed effects and R^2_c by the fixed and random effects for the phylogenetic mixed models.

Figure 5. Evolutionary correlations between hydraulic traits and between traits and environmental principal components (PC1, which is related to water availability; PC2, which is related to energy input and PC3, which is mainly related to soil depth). Environmental variables represent orthogonal PC axes and as such are not correlated. Lines represent significant evolutionary correlations (i.e., when the credible interval for the estimated correlation does not include zero), with the thickness of the line proportional to the strength of the correlation coefficient (also given on the same line). Light red lines represent negative relationships, dark blue lines indicate positive relationships. Significant correlation coefficients between traits when excluding environmental components and evolutionary affiliation as fixed effects are shown in italics, and significant correlation coefficients between traits including environmental components and evolutionary affiliation as fixed effects are shown in bold (in the case of the relationships between environmental axes and traits, only evolutionary affiliation was considered). Dashed lines represent evolutionary correlations that became non-significant when environmental effects and

641 major evolutionary affiliations were considered. Pie charts represent phylogenetic signal (dark),
642 inter-generic (medium) and intra-generic (light) variances reported in Table 1, calculated using the
643 maximum number of observations for each case. P-values are also displayed for each coefficient.
644 Signif. codes: '***': P < 0.001; '**': P < 0.01; '*': P < 0.05 '.': P < 0.1 ' ': P > 0.1.

645 **Figure 1**

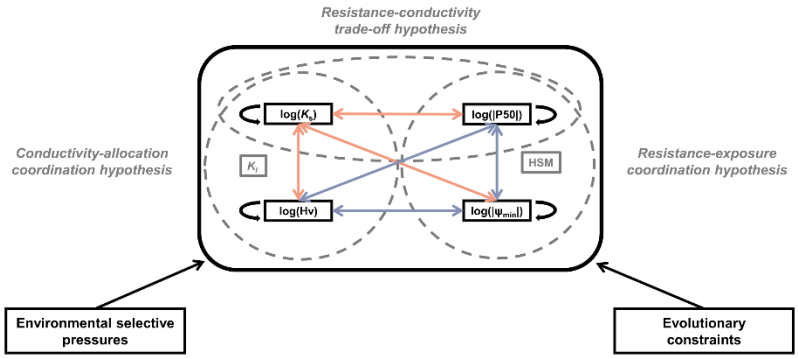

646

647 **Figure 2**

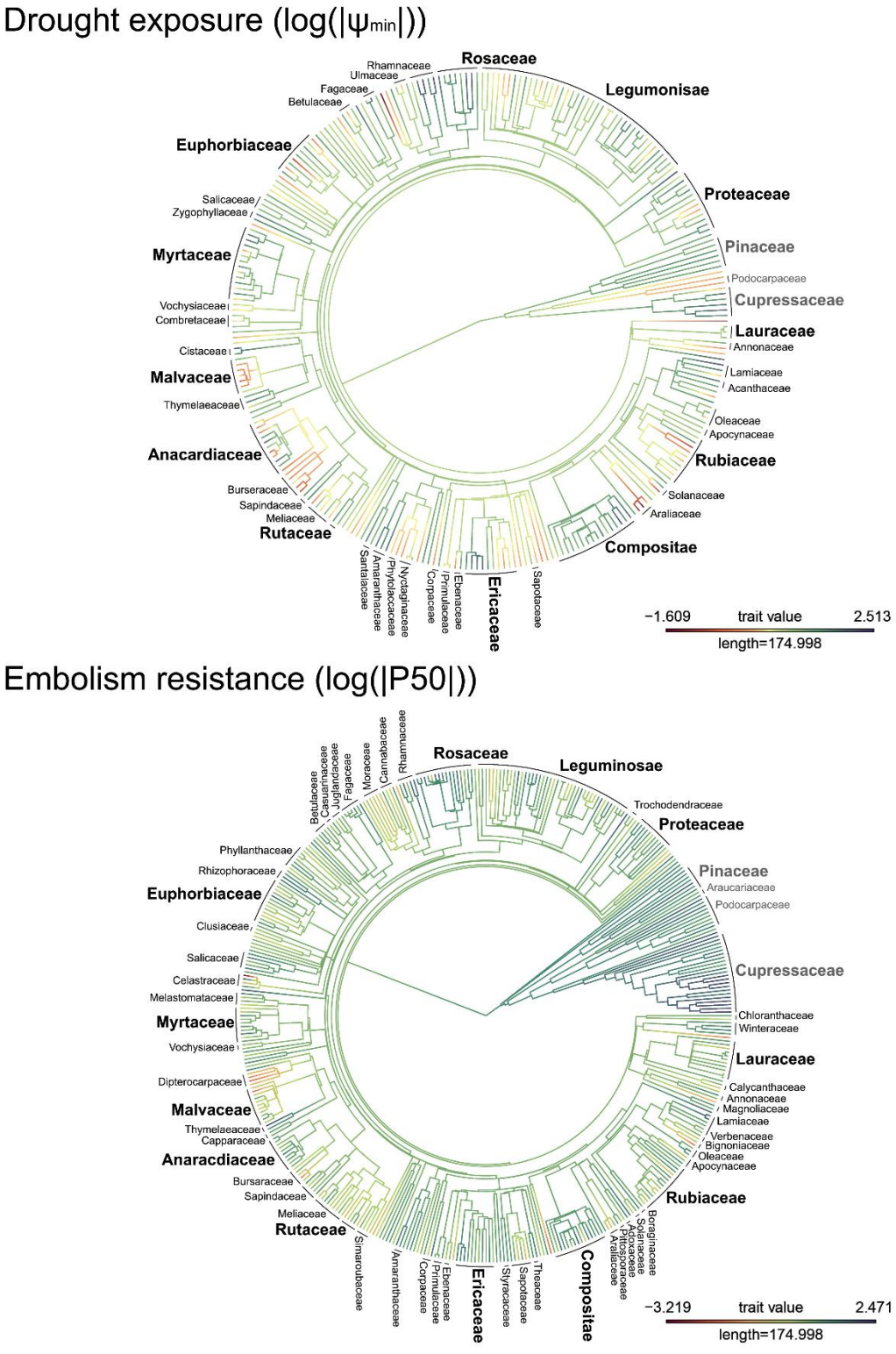

648

649 **Figure 3**

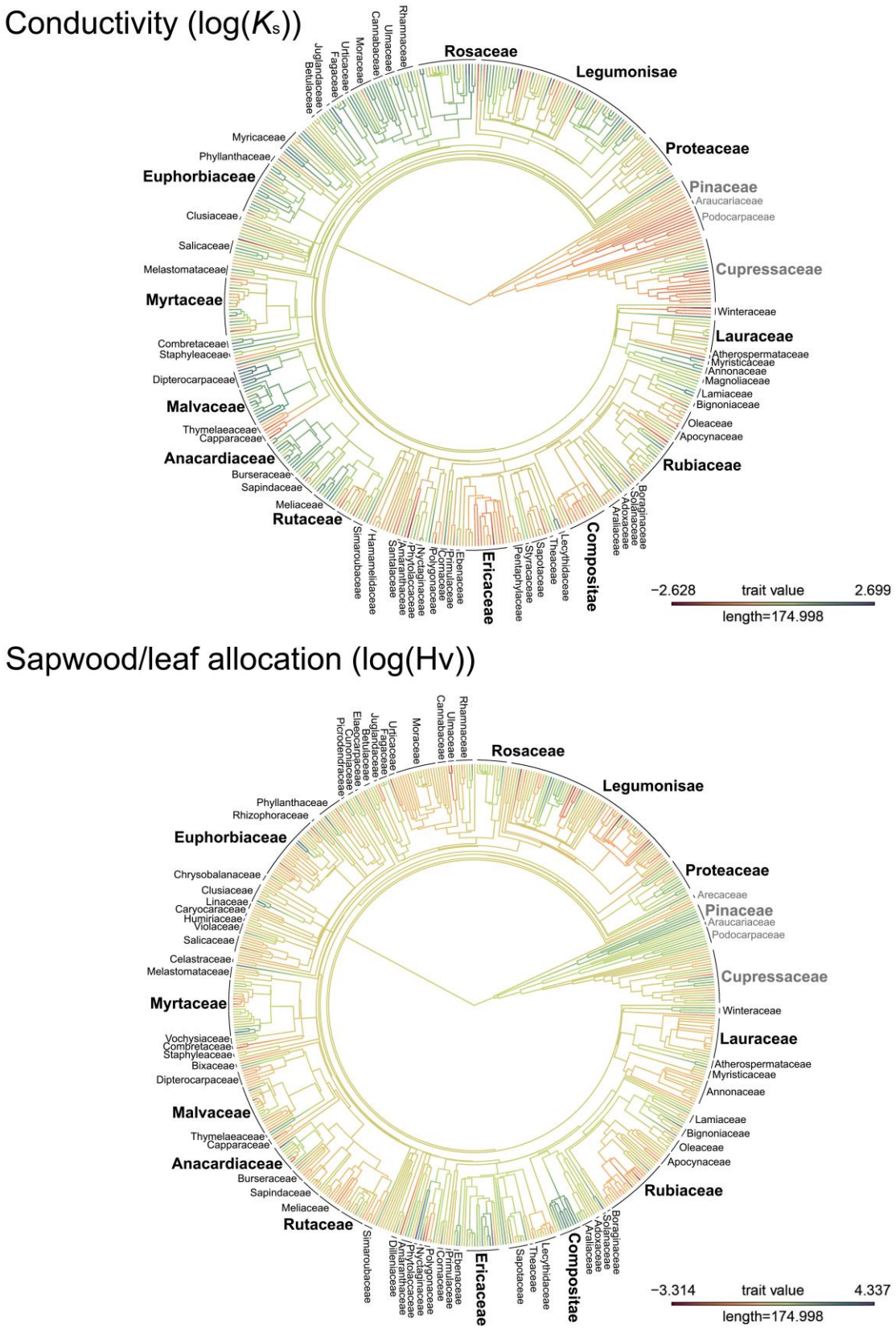
Conductivity (log(Ks))
Rosaceae
Legumonisae
Proteaceae
Pinaceae
Araucariaceae
Podocarpaceae
Cupressaceae
Winteraceae
Lauraceae
Atherospermataceae
Myristicaceae
Annonaceae
Magnoliaceae
Lamiaceae
Bignoniaceae
Oleaceae
Apocynaceae
Rubiaceae
Boraginaceae
Solanaceae
Adoxaceae
Araliaceae
Compositae
Lecythidaceae
Theaceae
Sapotaceae
Styracaceae
Pentaphylaceae
Ericaceae
Ebenaceae
Primulaceae
Polygonaceae
Nyctaginaceae
Phytolaccaceae
Amaranthaceae
Santalaceae
Hamamelidaceae
Simaroubaceae
Rutaceae
Meliaceae
Sapindaceae
Burseraceae
Anacardiaceae
Thymelaeaceae
Capparaceae
Malvaceae
Dipterocarpaceae
Combretaceae
Staphyleaceae
Myrtaceae
Melastomataceae
Salicaceae
Clusiaceae
Euphorbiaceae
Phyllanthaceae
Myricaceae
Betulaceae
Juglandaceae
Fagaceae
Urticaceae
Moraceae
Cannabaceae
Ulmaceae
Rhamnaceae
−2.628
trait value
2.699
length=174.998
Sapwood/leaf allocation (log(Hv))
Rosaceae
Legumonisae
Proteaceae
Arecaceae
Pinaceae
Araucariaceae
Podocarpaceae
Cupressaceae
Winteraceae
Lauraceae
Atherospermataceae
Myristicaceae
Annonaceae
Lamiaceae
Bignoniaceae
Oleaceae
Apocynaceae
Rubiaceae
Boraginaceae
Solanaceae
Adoxaceae
Araliaceae
Compositae
Lecythidaceae
Theaceae
Sapotaceae
Ericaceae
Ebenaceae
Primulaceae
Polygonaceae
Nyctaginaceae
Phytolaccaceae
Amaranthaceae
Dilleniaceae
Simaroubaceae
Rutaceae
Meliaceae
Sapindaceae
Burseraceae
Anacardiaceae
Thymelaeaceae
Capparaceae
Malvaceae
Dipterocarpaceae
Bixaceae
Staphyleaceae
Combretaceae
Vochysiaceae
Myrtaceae
Melastomataceae
Celastraceae
Salicaceae
Violaceae
Humiriaceae
Caryocaraceae
Linaceae
Clusiaceae
Chrysobalanaceae
Euphorbiaceae
Rhizophoraceae
Phyllanthaceae
Putranjivaceae
Elaeocarpaceae
Betulaceae
Juglandaceae
Fagaceae
Urticaceae
Moraceae
Cannabaceae
Ulmaceae
Rhamnaceae
−3.314
trait value
4.337
length=174.998

Figure 4

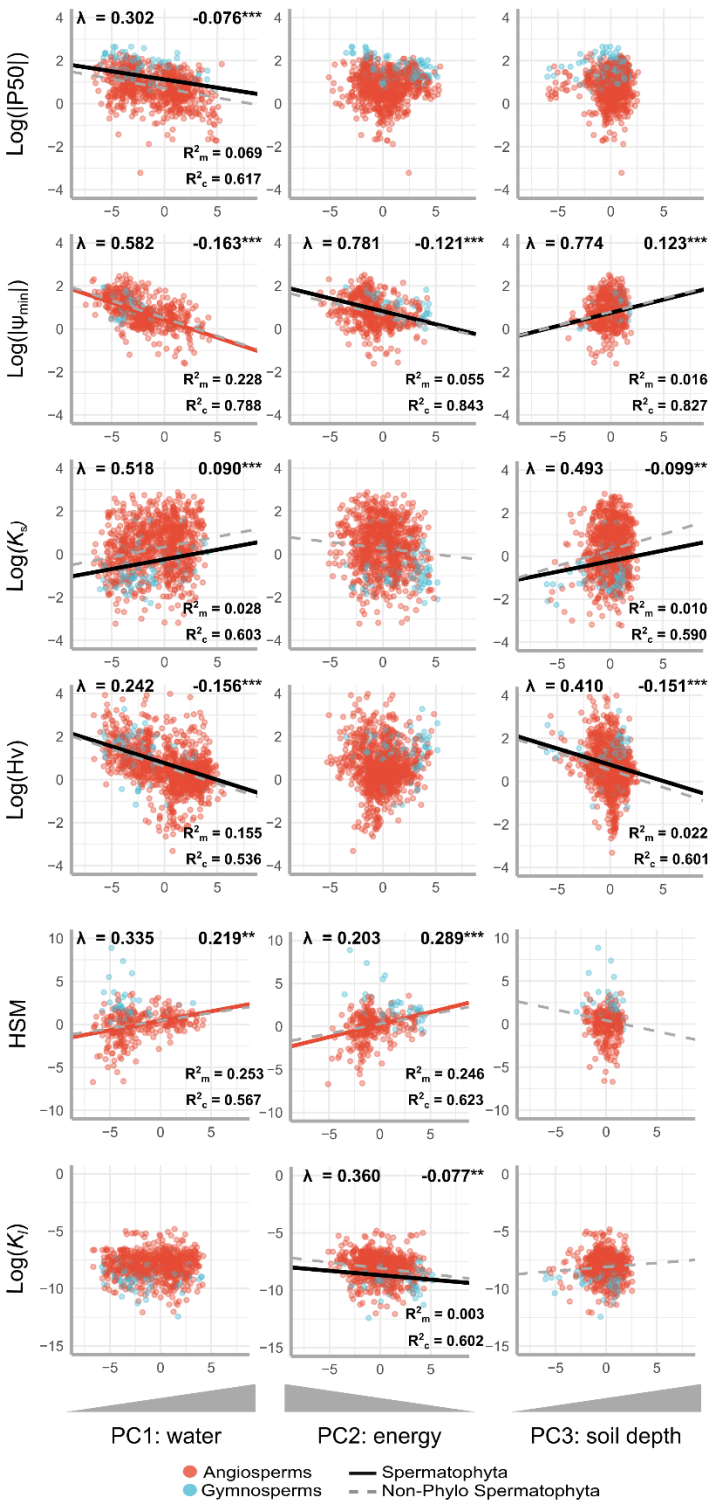
Log(|P50|)
Log(|ψmin|)
Log(Ks)
Log(Hv)
HSM
Log(Kl)
λ = 0.302 -0.076***
R²m = 0.069
R²c = 0.617
λ = 0.582 -0.163***
R²m = 0.228
R²c = 0.788
λ = 0.781 -0.121***
R²m = 0.055
R²c = 0.843
λ = 0.774 0.123***
R²m = 0.016
R²c = 0.827
λ = 0.518 0.090***
R²m = 0.028
R²c = 0.603
λ = 0.493 -0.099**
R²m = 0.010
R²c = 0.590
λ = 0.242 -0.156***
R²m = 0.155
R²c = 0.536
λ = 0.410 -0.151***
R²m = 0.022
R²c = 0.601
λ = 0.335 0.219**
R²m = 0.253
R²c = 0.567
λ = 0.203 0.289***
R²m = 0.246
R²c = 0.623
λ = 0.360 -0.077**
R²m = 0.003
R²c = 0.602
PC1: water
PC2: energy
PC3: soil depth
Angiosperms
Gymnosperms
Spermatophyta
Non-Phylo Spermatophyta

652 **Figure 5**

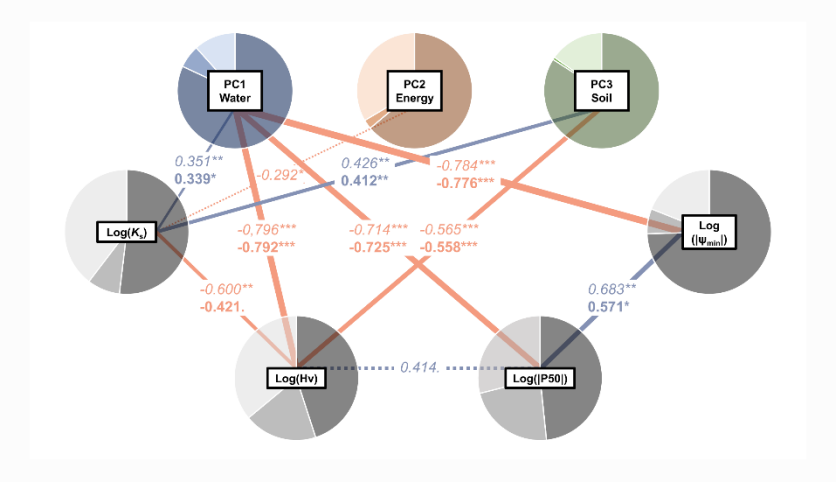

653

Supporting information

Figure S1. Whittaker diagrams.

Whittaker diagrams for all observations available (once matched with the phylogeny) and observations used for each one of the evolutionary correlations calculation (which has been restricted to those species with complete observations for the two traits and with genus-level phylogenetic information available).

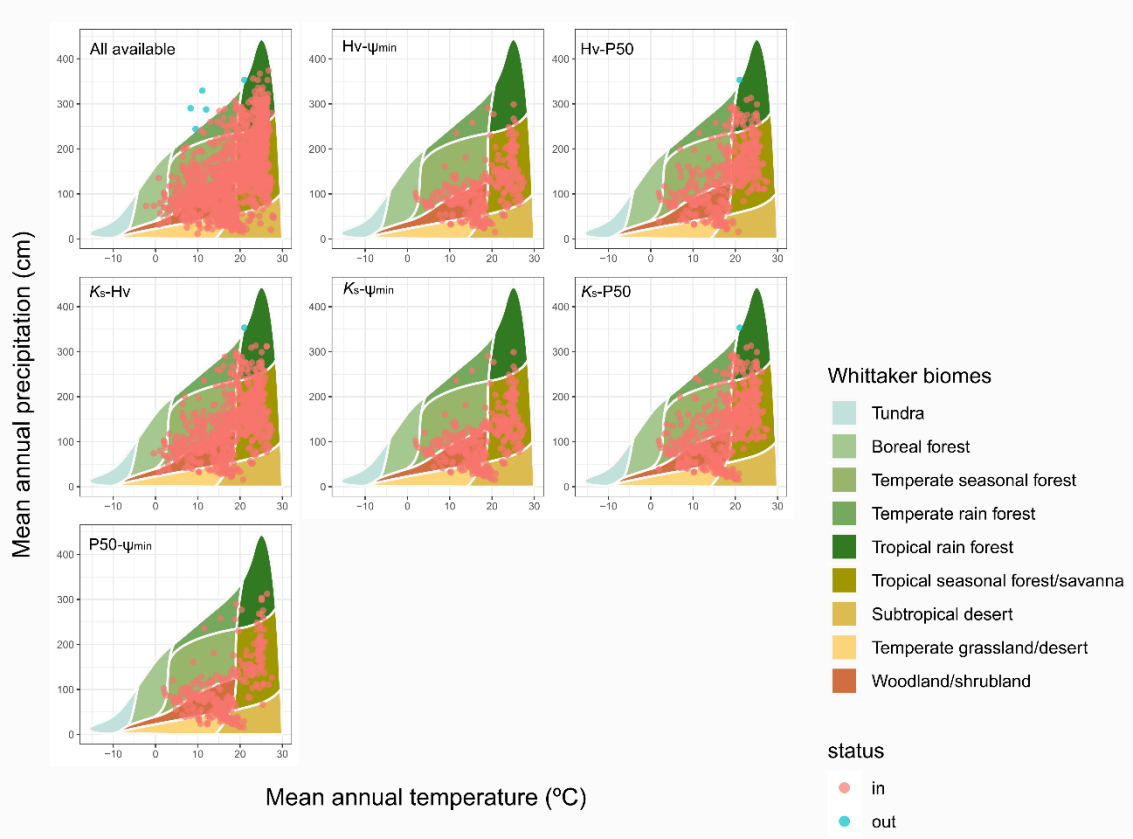

Figure S2. Geographic distribution of the three main environmental principal components. Species-mean coordinates are plotted for each species coloured by their environmental principal components mean values. Thus, some coordinates fall into the sea (presumably species present in both the Palearctic and the Nearctic realms). However, note that environmental variables were calculated for each occurrence of each species separately and then averaged to the species level. PC1 (a) is mainly related to water availability variables, PC2 (b) to energy input and PC3 (b) to soil depth (see Table S2 for a more concrete list of variables and their contribution to each of the three principal component).

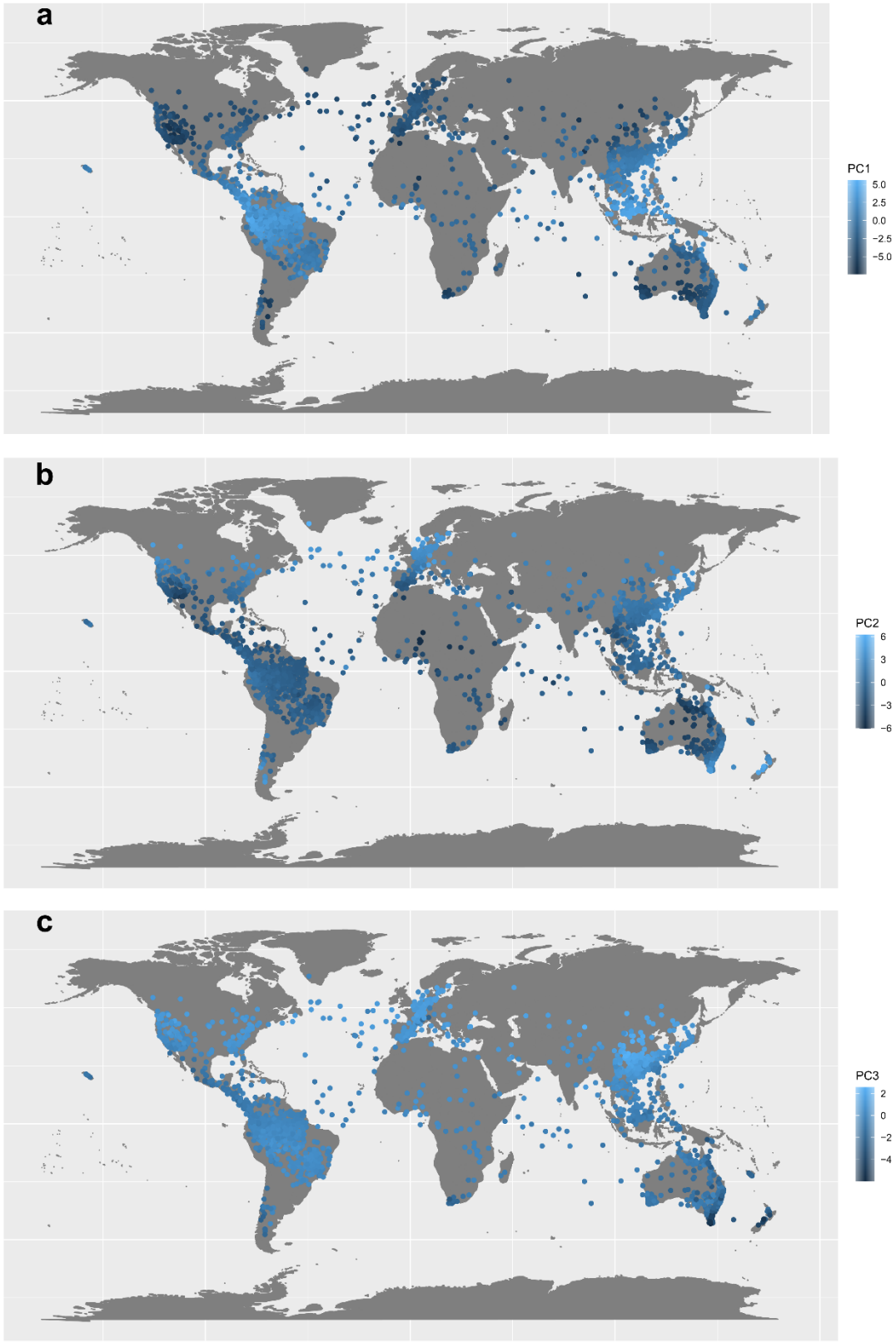

669

Figure S3. PCA biplot environment-hydraulic relationships.

PCA biplots showing the contributions of the 10 most important environmental variables to the first two principal components, PC1 and PC2 (a) and to PC1 and PC3 (b), colouring species as angiosperms (red circles) or gymnosperms (light blue triangles). Environmental variance explained for each principal component is shown in percentage. log(TS): temperature seasonality (log. transformed); pH: soil pH measured at 60 cm; VPD_{max}: maximum vapour pressure deficit; T_{max}: mean of the monthly maximum temperatures; MAT: mean annual temperature; Clay: clay content in percentage measured at 60cm, log(Wet P): Precipitation of the wettest month (log. Transformed); AP: annual precipitation; AI: aridity index (which is actually a moisture index); sqrt(DQ P): dry quarter precipitation (square root transformed); Soil depth: absolute depth to bedrock, SWC: soil water content at 200cm, $Wind_{max}$: mean of the monthly maximum wind velocity.

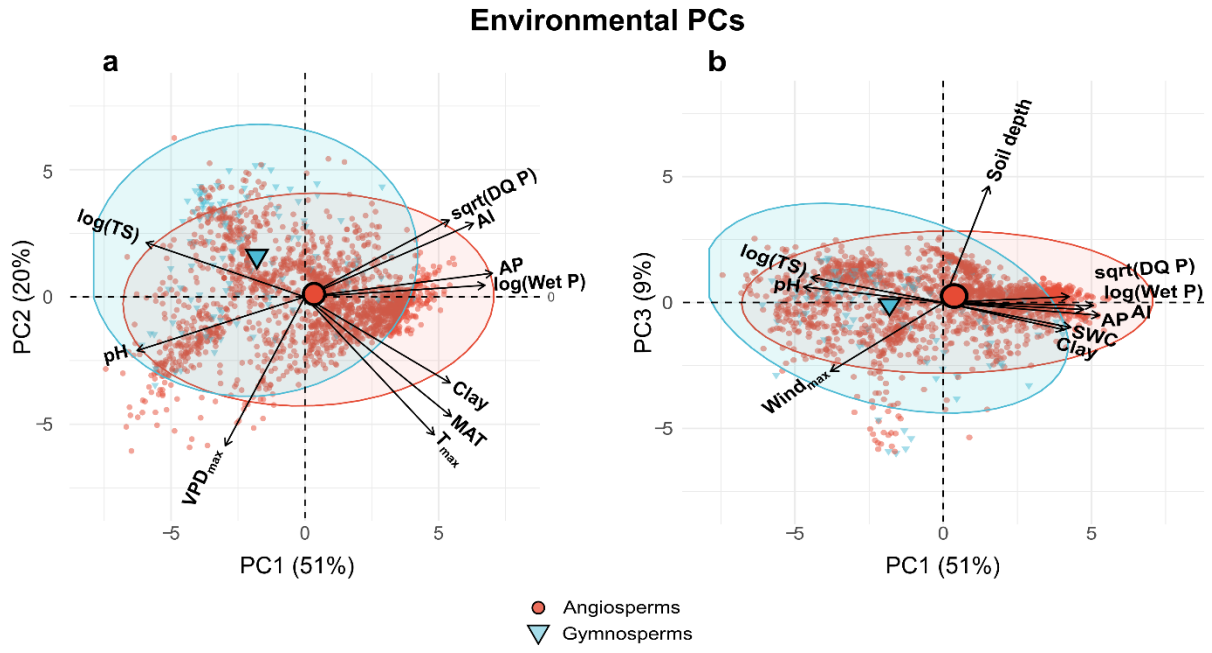

Figure S4. Phylogenetic reconstruction of Hydraulic Safety Margin (HSM) and leaf-specific hydraulic conductivity (log-transformed, log(K_l)) under a Brownian motion model of evolution.

Families with more than one genus are presented and some of the most important families are highlighted in bold. Gymnosperm families are displayed in grey and angiosperm ones in black.

Hydraulic Safety Margin (HSM)

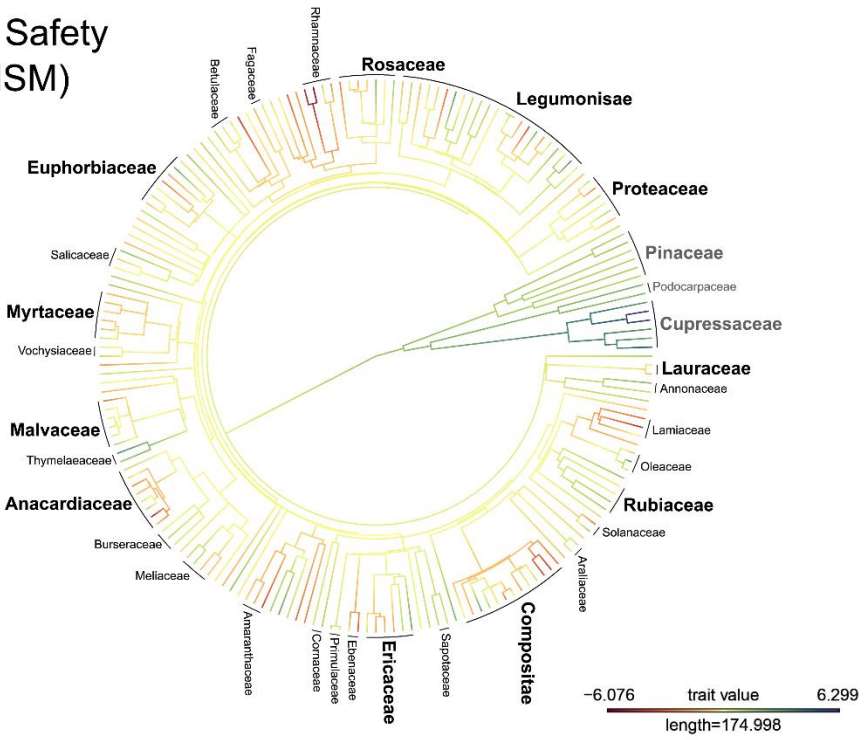

Leaf specific conductivity (log(K_l))

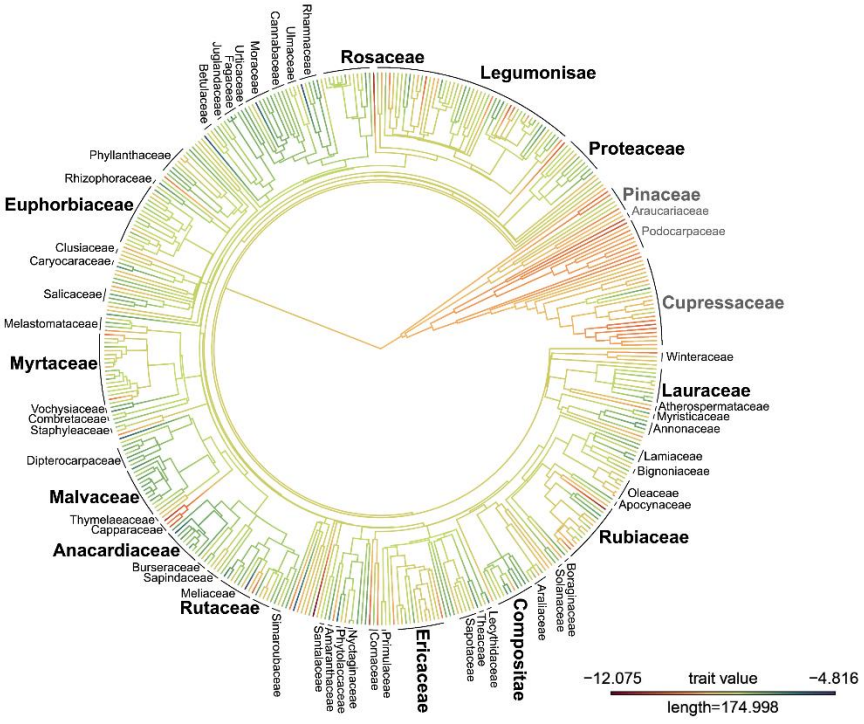

688

Figure S5. Phylogenetic reconstruction of the three environmental principal components under a Brownian motion model of evolution.

Families with more than one genus are presented and some of the most important families are highlighted in bold. Gymnosperm families are displayed in grey and angiosperm ones in black. PC1 refer to the first environmental principal component, representing variation in water availability and some related variables such as soil pH, soil clay content, soil water content and temperature seasonality, with high values characterizing more humid locations with leached acidic soils characteristic of tropical habitats. PC2 refer to the second environmental principal component, representing variation in energy input, with high values characterizing low solar irradiation, low maximum temperatures and low atmospheric water demand. PC3 refer to the third environmental principal component, largely reflected by soil depth and, to a lower extent, wind velocity, with high values indicating deeper soils with low sand content and low maximum wind velocities.

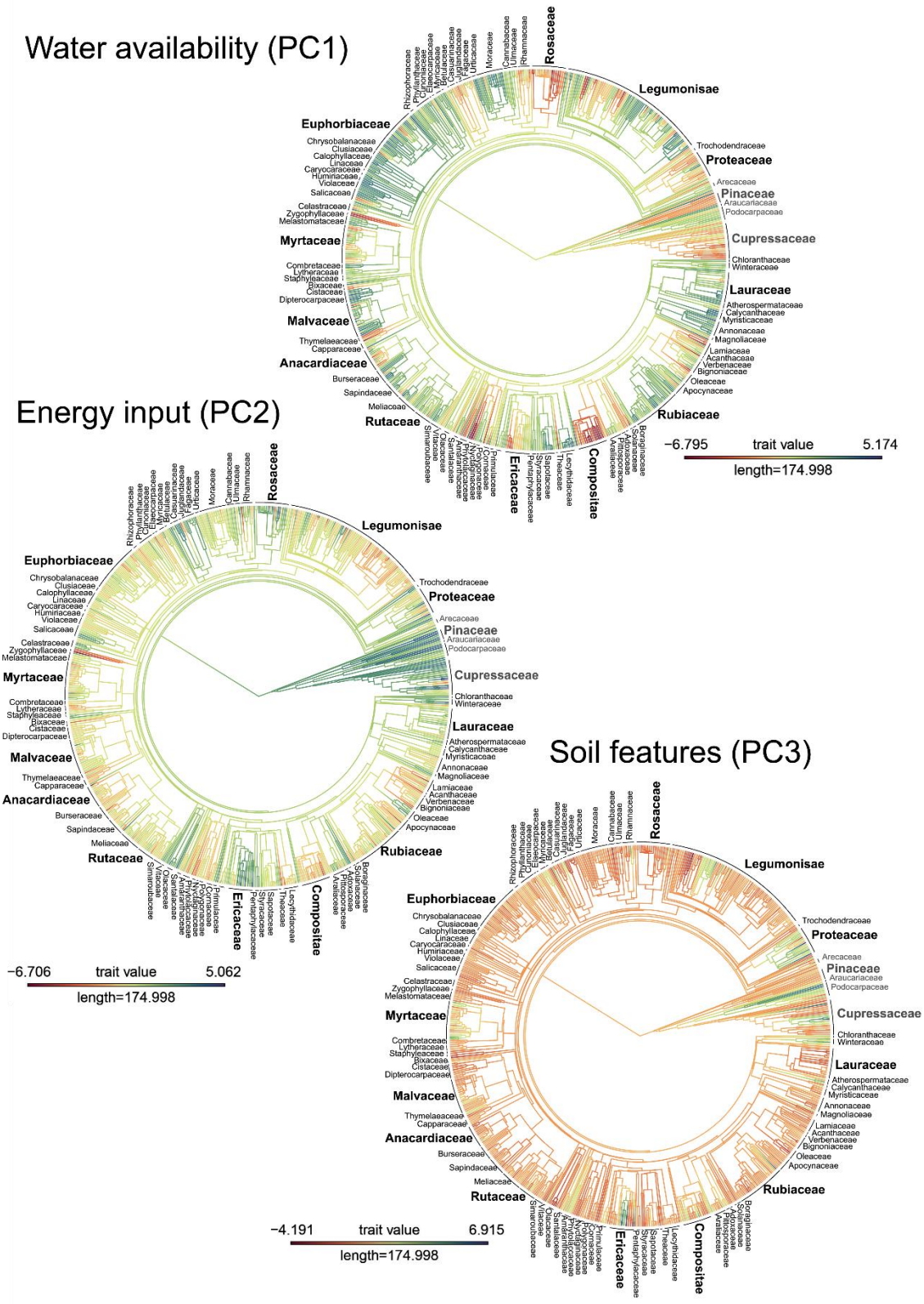
Water availability (PC1)
Rosaceae
Legumonisae
Euphorbiaceae
Proteaceae
Pinaceae
Cupressaceae
Lauraceae
Myrtaceae
Malvaceae
Anacardiaceae
Rutaceae
Rubiaceae
Ericaceae
Compositae
−6.795
trait value
5.174
length=174.998
Energy input (PC2)
Rosaceae
Legumonisae
Euphorbiaceae
Proteaceae
Pinaceae
Cupressaceae
Lauraceae
Myrtaceae
Malvaceae
Anacardiaceae
Rutaceae
Rubiaceae
Ericaceae
Compositae
−6.706
trait value
5.062
length=174.998
Soil features (PC3)
Rosaceae
Legumonisae
Euphorbiaceae
Proteaceae
Pinaceae
Cupressaceae
Lauraceae
Myrtaceae
Malvaceae
Anacardiaceae
Rutaceae
Rubiaceae
Ericaceae
Compositae
−4.191
trait value
6.915
length=174.998

Figure S6. Evolutionary correlations when using the species-level phylogeny.

Evolutionary correlations between hydraulic traits and between traits and environmental variables (environmental variables represent orthogonal PC axes and as such are not correlated) using a species-level phylogeny. Lines represent significant evolutionary correlations (i.e., when the credible interval for the estimated correlation do not include zero), with the thickness of the line proportional to the strength of the correlation coefficient (also given on the same line). Light red lines represent negative relationships, dark blue one's indicate positive relationships. Significant correlations coefficients between traits when excluding environmental effects and evolutionary affiliation as fixed effects are shown in italics, and significant correlation coefficients between traits including environmental effects and evolutionary affiliation as fixed effects are shown in bold (in the case of the relationships between environmental axis and traits, only evolutionary affiliation was considered). Dashed line represents evolutionary correlation that became non-significant when environmental effects and major evolutionary affiliations were considered. Pie charts represent phylogenetic (dark) and intraspecific (light) variances reported in Appendix 2 (i.e., calculated using the maximum number of observations for each case). P-values are also displayed for each coefficient. Signif. codes: '***': $P < 0.001$; '**': $P < 0.01$; '*': $P < 0.05$ '.': $P < 0.1$ ' ': $P > 0.1$.

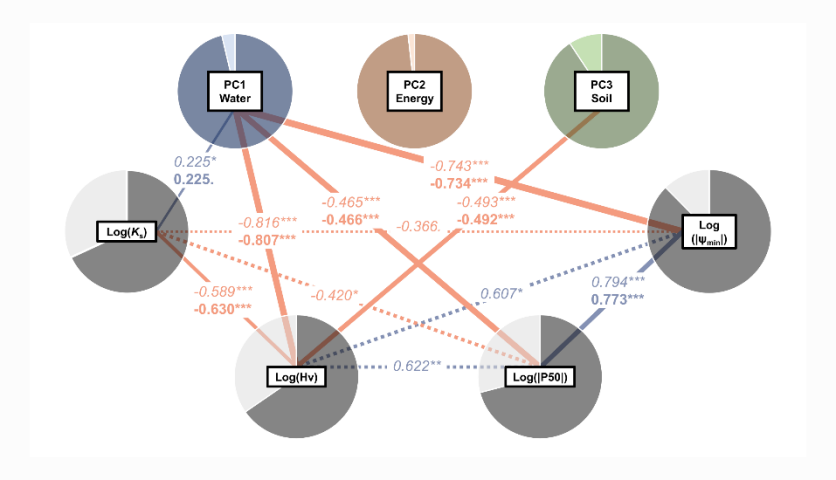
PC1
Water
PC2
Energy
PC3
Soil
Log(K_s)
Log
(|Ψ_{min}|)
Log(Hv)
Log(|P50|)
0.225*
0.225.
-0.743***
-0.734***
-0.465***
-0.466***
-0.493***
-0.492***
-0.816***
-0.807***
-0.366.
-0.589***
-0.630***
-0.420*
0.607*
0.794***
0.773***
0.622**

719

Figure S7. Gymnosperms observations for the relationships between HSM and ψ_{min} with PC1 and the one between HSM and PC2.

Species with HSM and ψ_{min} data available are shown coloured by family. PC1 refers to the environmental principal component mainly explained by water availability, PC2 refers to the principal component mainly explained by decreasing energy input.

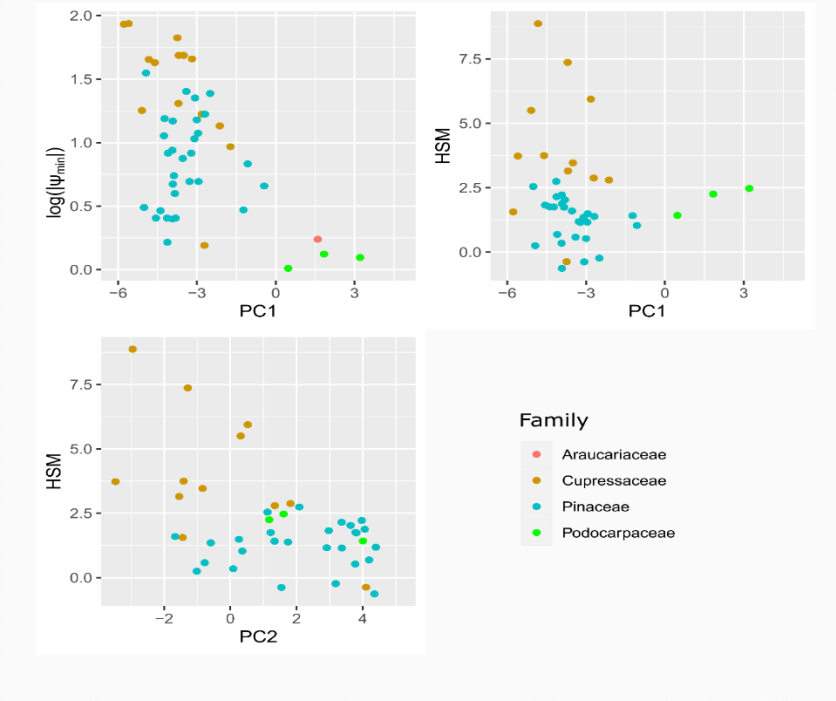

Table S1. Number of observations variables abbreviation and transformations.

Environmental variable and hydraulic traits nomenclature and number of whole dataset and major evolutionary affiliation observations. In the "Transformation" column data transformations are specified, when implemented.

Variable	Trasformation	Abbrebiation	Total observations	Angiosperms	Gymnosperms
Potential at the 50% loss of conductivity	Logaritmic of the absolute value	P50	894	771	123
Maximum stem-specific hydraulic conductivity	Logaritmic	K_s	1051	951	100
Leaf-specific hydraulic conductivity	Logaritmic	K_l	845	769	76
Huber value (sapwood area:leaf area ratio)	Logaritmic	Hv	1298	1223	75
Minimum water potential recorded	Logaritmic of the absolute value	ψ_{min}	553	505	48
Hydraulic Safety Margin (ψmin-P50)		HSM	336	294	42
Precipitation warmest quarter	Square root	sqrt(WQ P)	1937	1808	129
Precipitation wettest month	Logaritmic	log(Wet P)	1937	1808	129
Mean of the monthly maximum temperature		T_{max}	1937	1808	129
Temperature seasonality	Logaritmic	log(TS)	1937	1808	129
Annual precipitation		AP	1937	1808	129
Precipitation driest quarter	Square root	sqrt(DQ P)	1937	1808	129
Mean annual temperature		MAT	1937	1808	129
Aridity index (which is actually a moisture index)		AI	1937	1808	129
Solar radiation		srad	1937	1808	129
Mean of the monthly maximum wind velocity		$wind_{max}$	1937	1808	129
Maximum vapour pressure deficit		VPD_{max}	1937	1808	129
Absolute depth to bed rock		Soil depth	1937	1808	129
pH measured at 60cm		pH	1937	1808	129
Clay content in percentage measured at 60cm		Clay	1937	1808	129
Sand content in percentage measured at 60cm		Sand	1937	1808	129
Soil water content at 200cm		SWC	1937	1808	129

Table S2. Contribution of environmental variables to the three environmental principal components.

The highest contribution is highlighted for each variable. Sqrt(WQ P): Precipitation warmest quarter (square root transformed); log(Wet P): Precipitation wettest month (log. Transformed); T_{max}: Mean of the monthly maximum temperature; log(TS): Temperature seasonality (log. Transformed); AP: Annual precipitation; sqrt(DQ P): Precipitation driest quarter (square root Transformed); MAT: Mean annual temperature; AI: Aridity index (which is actually a moisture index); srad: Solar radiation; $Wind_{max}$: Mean of the monthly maximum wind velocity; VPD_{max}: Maximum vapour pressure deficit; Soil depth: Absolute depth to bedrock; pH: pH measured at 60cm; Clay: Clay content in percentage measured at 60cm; Sand: Sand content in percentage measured at 60cm; SWC: Soil water content at 200cm.

Variable	Contribution			Correlation		
	PC1	PC2	PC3	PC1	PC2	PC3
sqrt(WQ P)	**7.200**	2.273	0.125	0.766	0.269	0.042
log(Wet P)	**10.192**	0.121	0.031	0.912	0.062	-0.021
T_{max}	5.261	**16.947**	0.022	0.655	-0.734	-0.018
log(TS)	**7.906**	2.624	2.283	-0.803	0.289	0.181
AP	**11.069**	0.502	0.588	0.950	0.126	-0.092
sqrt(DQ P)	**6.551**	5.256	2.105	0.731	0.409	-0.174
MAT	6.749	**12.733**	0.041	0.742	-0.636	-0.024
AI	**8.932**	4.820	0.173	0.853	0.391	-0.050
srad	0.077	**20.291**	11.520	-0.079	-0.803	-0.406
$Wind_{max}$	5.767	3.142	**17.055**	-0.686	0.316	-0.495
VPD_{max}	1.986	**19.722**	0.920	-0.402	-0.792	0.115
Soil Depth	0.942	1.405	**48.430**	0.277	-0.211	0.833
pH	**8.843**	2.569	0.873	-0.849	-0.286	0.112
Clay	**6.636**	6.592	2.668	0.736	-0.458	-0.196
Sand	4.496	0.825	**10.945**	-0.606	-0.162	-0.396
SWC	**7.393**	0.178	2.220	0.776	0.075	-0.178

Table S3. Reference table for all the models reported in the main text.

All models were implemented with and without accounting for the phylogeny. In the fixed structure column, variables to the right of the "~" symbol are response variables, those to the left are predictors. Abbreviations: "env"(1): individual environmental principal component; env(3): three main environmental principal components; trait: individual hydraulic trait; Affiliation: major evolutionary affiliation (angiosperm or gymnosperm), "1" refer to the intercept.

Fixed structure	Description	Phylogeny used	Number of response variables	Results Ref.
env(1) ~ 1	Phylogenetic signal	Genus-level	Uni-response	Table 1, Fig. 4 (pie charts)
trait ~ 1		Genus-level	Uni-response	Table 1, Fig. 4 (pie charts)
trait ~ env(1)	Uni-response environment models	Genus-level	Uni-response	Fig. 4, Table S5
trait ~ env(1) + Affiliation		Genus-level	Uni-response	Fig. 4, Table S5
trait ~ env(1) * Affiliation		Genus-level	Uni-response	Fig. 4, Table S5
trait , env(1) ~ 1	Evolutionary correlations	Genus-level	Bi-response	Fig. 5, Table S6
trait , env(1) ~ 1 + Affiliation		Genus-level	Bi-response	Fig. 5, Table S6
trait , trait ~ 1		Genus-level	Bi-response	Fig. 5, Table S6
trait , trait ~ 1 + Affiliation		Genus-level	Bi-response	Fig. 5, Table S6
trait , trait ~ 1 + env(3)		Genus-level	Bi-response	Fig. 5, Table S6
trait , trait ~ 1 + env(3) + Affiliation		Genus-level	Bi-response	Fig. 5, Table S6

trait , trait ~ 1 + env(3) * Affiliation		Genus-level	Bi-response	Fig. 5, Table S6
env(1) ~ 1	Phylogenetic signal	Species-level	Uni-response	Appendix 2, Fig. S6
trait ~ 1		Species-level	Uni-response	Appendix 2, Fig. S6
trait , env(1) ~ -1	Evolutionary correlations	Species-level	Bi-response	Appendix 2, Fig. S6
trait , env(1) ~ -1 + Affiliation		Species-level	Bi-response	Appendix 2, Fig. S6
trait , trait ~ -1		Species-level	Bi-response	Appendix 2, Fig. S6
trait , trait ~ -1 + env(3) * Affiliation		Species-level	Bi-response	Appendix 2, Fig. S6

747

Table S4. Non-phylogenetic model's variance partition.

Mean non-phylogenetic inter-generic (γ) and non-phylogenetic intra-generic (ρ) variance in non-phylogenetic models without fixed effects. Note that phylogenetic variance (λ) is 0, as the phylogenetic effect was not considered.

variable	Phylogenetic (λ)	Inter-generic (γ)	Intra-generic (ρ)
HSM	0	0.490	0.510
Log(Hv)	0	0.514	0.486
Log(K_l)	0	0.280	0.720
Log(K_s)	0	0.459	0.541
Log($\lvert\psi_{min}\rvert$)	0	0.621	0.379
Log(|P50|)	0	0.636	0.364
PC1	0	0.787	0.213
PC2	0	0.483	0.517
PC3	0	0.641	0.359

Table S5. Uni-response models description.

DICs and explained variances for phylogenetic and non-phylogenetic uni-response models. The fixed formula is shown in each case. DICs for the phylogenetic models are shown. "NP" refer to non-phylogenetic models (i.e., only including genus contingency as random effect) explained variances. R2c refer to the conditional and R2m refers to the marginal explained variances. Abbreviations: K_s: Xylem conductivity; P50: xylem resistance to embolism; Hv: sapwood allocation relative to leaf area; ψ_{min}: drought exposure, HSM: hydraulic safety margin; K_l: and sufficiency; PC1: water availability; PC2: energy input and PC3: soil depth; Affiliation: evolutionary affiliation (angiosperm or gymnosperm).

Fixed effects formula	DIC	R2m	R2c	NP R2m	NP R2c
HSM ~ 1	1181	0	0.612	0	0.49
HSM ~ PC1 * Affiliation	1133	0.253	0.657	0.301	0.554
HSM ~ PC1 + Affiliation	1138	0.211	0.647	0.268	0.535
HSM ~ PC1	1139	0.065	0.625	0.026	0.519
HSM ~ PC2 * Affiliation	1133	0.246	0.623	0.28	0.509
HSM ~ PC2 + Affiliation	1142	0.184	0.658	0.237	0.54
HSM ~ PC2	1143	0.035	0.619	0.031	0.495
HSM ~ PC3 * Affiliation	1146	0.172	0.624	0.23	0.542
HSM ~ PC3 + Affiliation	1147	0.176	0.634	0.235	0.541
HSM ~ PC3	1150	0.006	0.618	0.02	0.528
log_Hv ~ 1	3147	0	0.641	0	0.514
log_Hv ~ PC1 + Affiliation	3013	0.166	0.549	0.187	0.479
log_Hv ~ PC1	3013	0.155	0.536	0.184	0.477
log_Hv ~ PC1 * Affiliation	3014	0.168	0.551	0.188	0.478
log_Hv ~ PC2 * Affiliation	3058	0.028	0.662	0.014	0.51
log_Hv ~ PC2	3060	0.002	0.646	0.001	0.509
log_Hv ~ PC2 + Affiliation	3060	0.028	0.657	0.013	0.509
log_Hv ~ PC3 + Affiliation	3066	0.045	0.615	0.04	0.477
log_Hv ~ PC3	3066	0.022	0.601	0.032	0.48
log_Hv ~ PC3 * Affiliation	3068	0.045	0.614	0.043	0.475
log_K_l ~ 1	2348	0	0.47	0	0.28
log_K_l ~ PC1 * Affiliation	2250	0.067	0.482	0.077	0.299
log_K_l ~ PC1	2252	0.002	0.447	0.002	0.282
log_K_l ~ PC1 + Affiliation	2254	0.069	0.463	0.077	0.296

log_K_l ~ PC2	2250	0.016	0.41	0.033	0.254
log_K_l ~ PC2 * Affiliation	2251	0.089	0.439	0.093	0.283
log_K_l ~ PC2 + Affiliation	2251	0.084	0.434	0.088	0.276
log_K_l ~ PC3	2250	0.002	0.454	0.008	0.297
log_K_l ~ PC3 + Affiliation	2252	0.072	0.462	0.077	0.304
log_K_l ~ PC3 * Affiliation	2253	0.075	0.47	0.077	0.304
log_K_s ~ 1	2795	0	0.608	0	0.459
log_K_s ~ log_Hv	2079	0.116	0.614	0.181	0.494
log_K_s ~ log_Hv * Affiliation	2081	0.166	0.64	0.23	0.506
log_K_s ~ log(|P50|)	1581	0.041	0.634	0.074	0.499
log_K_s ~ log(|P50|) * Affiliation	1583	0.111	0.666	0.118	0.51
log_K_s ~ PC1	2670	0.028	0.603	0.042	0.475
log_K_s ~ PC1 + Affiliation	2670	0.084	0.631	0.089	0.479
log_K_s ~ PC1 * Affiliation	2670	0.091	0.635	0.09	0.479
log_K_s ~ PC2	2694	0.003	0.602	0.01	0.447
log_K_s ~ PC2 + Affiliation	2694	0.057	0.623	0.055	0.453
log_K_s ~ PC2 * Affiliation	2696	0.058	0.625	0.056	0.456
log_K_s ~ PC3	2685	0.01	0.59	0.028	0.462
log_K_s ~ PC3 + Affiliation	2685	0.063	0.618	0.069	0.462
log_K_s ~ PC3 * Affiliation	2687	0.062	0.617	0.07	0.463
log(|ψ_{min}|) ~ 1	828	0	0.812	0	0.621
log(|ψ_{min}|) ~ log(|P50|)	431	0.279	0.738	0.299	0.71
log(|ψ_{min}|) ~ log(|P50|) * Affiliation	432	0.29	0.738	0.314	0.703
log(|ψ_{min}|) ~ PC1 * Affiliation	688	0.228	0.788	0.303	0.686
log(|ψ_{min}|) ~ PC1	692	0.211	0.763	0.302	0.679
log(|ψ_{min}|) ~ PC1 + Affiliation	692	0.229	0.781	0.302	0.68
log(|ψ_{min}|) ~ PC2 * Affiliation	724	0.099	0.854	0.107	0.692
log(|ψ_{min}|) ~ PC2	725	0.055	0.843	0.094	0.691
log(|ψ_{min}|) ~ PC2 + Affiliation	725	0.099	0.854	0.104	0.687
log(|ψ_{min}|) ~ PC3 + Affiliation	793	0.07	0.841	0.047	0.649
log(|ψ_{min}|) ~ PC3	793	0.016	0.827	0.036	0.644
log(|ψ_{min}|) ~ PC3 * Affiliation	795	0.072	0.841	0.051	0.65
log(|P50|) ~ 1	1426	0	0.71	0	0.636
log(|P50|) ~ PC1 * Affiliation	1396	0.193	0.635	0.23	0.605
log(|P50|) ~ PC1	1397	0.069	0.617	0.097	0.588
log(|P50|) ~ PC1 + Affiliation	1397	0.194	0.636	0.231	0.606
log(|P50|) ~ PC2 * Affiliation	1402	0.116	0.725	0.148	0.635
log(|P50|) ~ PC2 + Affiliation	1403	0.108	0.719	0.141	0.631
log(|P50|) ~ PC2	1403	0.001	0.694	0.002	0.623
log(|P50|) ~ PC3 * Affiliation	1394	0.107	0.728	0.141	0.637
log(|P50|) ~ PC3 + Affiliation	1397	0.105	0.725	0.144	0.636

log(|P50|) ~ PC3	1397	0.003	0.699	0.002	0.628
PC1 ~ 1	6985	0	0.891	0	0.787
PC2 ~ 1	6723	0	0.697	0	0.483
PC3 ~ 1	4707	0	0.85	0	0.641

761 **Table S6. Evolutionary correlations and DICs for bi-response models.**

762 Mean of the evolutionary correlation (Cor), credible interval (lower and upper HDP) and p-value
763 reported by bi-response models. The fixed formula is shown in each case. Models are ordered by
764 DIC values (from lower to higher) for each set of nested models (same response variables).
765 Statistically significant evolutionary correlations are highlighted in bold and marginally significant
766 in italics. Abbreviations: K_s: Xylem conductivity; P50: xylem resistance to embolism; Hv:
767 sapwood allocation relative to leaf area; ψ_{min}: drought exposure, HSM: hydraulic safety margin;
768 K_l: and sufficiency; PC1: water availability; PC2: energy input and PC3: soil depth; Affiliation:
769 evolutionary affiliation (angiosperm or gymnosperm).

Var. 1	Var. 2	Fixed formula	Cor	Lower HDP	Upper HDP	p-value	DIC
log(Hv)	log(|ψ_{min}|)	(log(Hv), log(|ψ_{min}|)) ~ 1 + (PC1 + PC2 + PC3) * :Affiliation	-0.094	-0.681	0.436	0.752	1403
log(Hv)	log(|ψ_{min}|)	(log(Hv), log(|ψ_{min}|)) ~ 1 + PC1 + PC2 + PC3	-0.100	-0.636	0.486	0.736	1403
log(Hv)	log(|ψ_{min}|)	(log(Hv), log(|ψ_{min}|)) ~ 1 + Affiliation + PC1 + PC2 + PC3	-0.117	-0.624	0.462	0.664	1404
log(Hv)	log(|ψ_{min}|)	(log(Hv), log(|ψ_{min}|)) ~ 1 + Affiliation	0.222	-0.405	0.801	0.494	1571
log(Hv)	log(|ψ_{min}|)	(log(Hv), log(|ψ_{min}|)) ~ 1	0.217	-0.405	0.798	0.509	1571
log(Hv)	**PC1**	**(log(Hv), PC1) ~ 1**	**-0.796**	**-0.913**	**-0.662**	**0.000**	**7475**
log(Hv)	**PC1**	**(log(Hv), PC1) ~ 1 + Affiliation**	**-0.792**	**-0.910**	**-0.657**	**0.000**	**7475**
log(Hv)	PC2	(log(Hv), PC2) ~ 1 + Affiliation	0.145	-0.160	0.462	0.397	7296
log(Hv)	PC2	(log(Hv), PC2) ~ 1	0.156	-0.141	0.473	0.363	7296
log(Hv)	**PC3**	**(log(Hv), PC3) ~ 1 + Affiliation**	**-0.558**	**-0.747**	**-0.363**	**0.000**	**5971**
log(Hv)	**PC3**	**(log(Hv), PC3) ~ 1**	**-0.565**	**-0.737**	**-0.367**	**0.000**	**5972**
log(K_s)	*log(Hv)*	*(log(K_s)_log(Hv)) ~ 1 + PC1 + PC2 + PC3*	*-0.423*	*-0.805*	*-0.016*	*0.077*	*3843*
log(K_s)	*log(Hv)*	*(log(K_s)_log(Hv)) ~ 1* + Affiliation + *PC1 + PC2 + PC3*	*-0.423*	*-0.795*	*-0.005*	*0.079*	*3843*
log(K_s)	*log(Hv)*	*cbind(log_(K_s)_log(Hv)) ~ 1 + (PC1 + PC2 + PC3) ** Affiliation	*-0.421*	*-0.827*	*-0.012*	*0.085*	*3853*
log(K_s)	**log(Hv)**	**(log(K_s), log(Hv)) ~ 1**	**-0.600**	**-0.868**	**-0.271**	**0.008**	**4058**
log(K_s)	**log(Hv)**	**(log(K_s), log(Hv)) ~ 1 + Affiliation**	**-0.588**	**-0.879**	**-0.247**	**0.010**	**4059**
log(K_s)	log(|ψ_{min}|)	(log(K_s), log(|ψ_{min}|)) ~ 1 + (PC1 + PC2 + PC3) * Affiliation	0.019	-0.538	0.566	0.934	1571
log(K_s)	log(|ψ_{min}|)	(log(K_s), log(|ψ_{min}|)) ~ 1 + Affiliation + PC1 + PC2 + PC3	-0.013	-0.535	0.569	0.966	1572
log(K_s)	log(|ψ_{min}|)	(log(K_s), log(|ψ_{min}|)) ~ 1 + PC1 + PC2 + PC3	0.008	-0.512	0.555	0.970	1572

log(K_s)	log($\|\psi_{min}\|$)	(log(K_s), log($\|\psi_{min}\|$)) ~ 1	-0.080	-0.683	0.487	0.785	1768
log(K_s)	log($\|\psi_{min}\|$)	(log(K_s), log($\|\psi_{min}\|$)) ~ 1 + Affiliation	-0.066	-0.675	0.507	0.823	1768
log(K_s)	log(|P50|)	(log(K_s), log(|P50|)) ~ 1 + Affiliation + PC1 + PC2 + PC3	-0.046	-0.517	0.399	0.851	2489
log(K_s)	log(|P50|)	(log(K_s), log(|P50|)) ~ 1 + PC1 + PC2 + PC3	-0.098	-0.510	0.324	0.648	2489
log(K_s)	log(|P50|)	(log(K_s), log(|P50|)) ~ 1 + (PC1 + PC2 + PC3) * Affiliation	-0.019	-0.475	0.408	0.917	2495
log(K_s)	log(|P50|)	(log(K_s), log(|P50|)) ~ 1	-0.317	-0.665	0.055	0.114	2596
log(K_s)	log(|P50|)	(log(K_s), log(|P50|)) ~ 1 + Affiliation	-0.274	-0.639	0.165	0.211	2596
log(K_s)	**PC1**	**(log(K_s), PC1) ~ 1 + Affiliation**	**0.339**	**0.093**	**0.578**	**0.010**	**6343**
log(K_s)	**PC1**	**(log(K_s), PC1) ~ 1**	**0.351**	**0.110**	**0.594**	**0.009**	**6343**
log(K_s)	PC2	(log(K_s), PC2) ~ 1 + Affiliation	-0.275	-0.570	0.003	0.069	6315
log(K_s)	*PC2*	*(log(K_s), PC2) ~ 1*	*-0.292*	*-0.576*	*-0.007*	*0.048*	*6315*
log(K_s)	**PC3**	**(log(K_s), PC3) ~ 1 + Affiliation**	**0.412**	**0.144**	**0.683**	**0.008**	**5216**
log(K_s)	**PC3**	**(log(K_s), PC3) ~ 1**	**0.426**	**0.185**	**0.706**	**0.005**	**5216**
log($\|\psi_{min}\|$)	**PC1**	**(log($\|\psi_{min}\|$), PC1) ~ 1 + Affiliation**	**-0.776**	**-0.908**	**-0.624**	**0.000**	**2636**
log($\|\psi_{min}\|$)	**PC1**	**(log($\|\psi_{min}\|$), PC1) ~ 1**	**-0.784**	**-0.907**	**-0.620**	**0.000**	**2636**
log($\|\psi_{min}\|$)	PC2	(log($\|\psi_{min}\|$), PC2) ~ 1	-0.232	-0.566	0.129	0.214	2744
log($\|\psi_{min}\|$)	PC2	(log($\|\psi_{min}\|$), PC2) ~ 1 + Affiliation	-0.249	-0.594	0.124	0.195	2745
log($\|\psi_{min}\|$)	PC3	(log($\|\psi_{min}\|$), PC3) ~ 1 + Affiliation	0.115	-0.236	0.452	0.539	1916
log($\|\psi_{min}\|$)	PC3	(log($\|\psi_{min}\|$), PC3) ~ 1	0.126	-0.208	0.480	0.471	1917
log(|P50|)	log(Hv)	(log(|P50|), log(Hv)) ~ 1 + PC1 + PC2 + PC3	0.060	-0.423	0.507	0.818	1834
log(|P50|)	log(Hv)	(log(|P50|), log(Hv)) ~ 1 + Affiliation + PC1 + PC2 + PC3	0.061	-0.413	0.511	0.779	1835
log(|P50|)	log(Hv)	(log(|P50|), log(Hv)) ~ 1 + (PC1 + PC2 + PC3) * Affiliation	0.053	-0.404	0.531	0.831	1843
log(|P50|)	*log(Hv)*	*(log(|P50|), log(Hv)) ~ 1*	*0.414*	*0.052*	*0.790*	*0.070*	*1927*
log(|P50|)	log(Hv)	(log(|P50|), log(Hv)) ~ 1 + Affiliation	0.385	-0.043	0.777	0.121	1927
log(|P50|)	**log($\|\psi_{min}\|$)**	**(log(|P50|), log($\|\psi_{min}\|$)) ~ 1 + (PC1 + PC2 + PC3) * Affiliation**	**0.571**	**0.213**	**0.860**	**0.015**	**745**
log(|P50|)	**log($\|\psi_{min}\|$)**	**(log(|P50|), log($\|\psi_{min}\|$)) ~ 1 + Affiliation + PC1 + PC2 + PC3**	**0.552**	**0.168**	**0.863**	**0.030**	**751**
log(|P50|)	**log($\|\psi_{min}\|$)**	**(log(|P50|), log($\|\psi_{min}\|$)) ~ 1 + PC1 + PC2 + PC3**	**0.556**	**0.168**	**0.833**	**0.015**	**751**
log(|P50|)	**log($\|\psi_{min}\|$)**	**(log(|P50|), log($\|\psi_{min}\|$)) ~ 1 + Affiliation**	**0.702**	**0.428**	**0.917**	**0.000**	**834**
log(|P50|)	**log($\|\psi_{min}\|$)**	**(log(|P50|), log($\|\psi_{min}\|$)) ~ 1**	**0.683**	**0.386**	**0.914**	**0.006**	**834**
log(|P50|)	**PC1**	**(log(|P50|), PC1) ~ 1 + Affiliation**	**-0.725**	**-0.885**	**-0.537**	**0.000**	**4476**
log(|P50|)	**PC1**	**(log(|P50|), PC1) ~ 1**	**-0.714**	**-0.875**	**-0.524**	**0.000**	**4477**
log(|P50|)	PC2	(log(|P50|), PC2) ~ 1	0.050	-0.316	0.460	0.803	4487
log(|P50|)	PC2	(log(|P50|), PC2) ~ 1 + Affiliation	0.015	-0.344	0.400	0.978	4488
log(|P50|)	PC3	(log(|P50|), PC3) ~ 1 + Affiliation	-0.110	-0.456	0.208	0.570	3677
log(|P50|)	PC3	(log(|P50|), PC3) ~ 1	-0.097	-0.426	0.229	0.573	3678

Appendix S1. Supplementary methods.

Phylogenetic mixed model description

Phylogenetic mixed models are commonly used in quantitative genetics (the so called "animal" model), being useful for comparative analyses as they allow to incorporate a range of variance structures for the random effects, including shared ancestry through a phylogeny (Housworth *et al.* 2004). The general model structure is defined as follows:

$$y = \mu + \beta x + p + g + e \quad (1)$$

Were μ is the grand mean, interpreted as the root ancestor state, β is the slope for the covariate x (fixed effect, in green), p and g are the variability caused by the genus-level phylogeny and the genus contingency effects (random effects, in red), and e is the residual error (Housworth *et al.* 2004; Villemereuil & Nakagawa 2014). Both fixed (β) and random (r, which is $p + g$) effects and the residuals (e) are expected to come from a multivariate normal distribution as it follows:

$$\begin{bmatrix} \beta \\ r \\ e \end{bmatrix} \sim N\left(\begin{bmatrix} \beta_0 \\ 0 \\ 0 \end{bmatrix}, \begin{bmatrix} B & 0 & 0 \\ 0 & G & 0 \\ 0 & 0 & R \end{bmatrix}\right) \quad (2)$$

Where β is the fixed effect parameter to estimate, β_0 is the prior means for the fixed effects with prior (co)variance matrix B, and G and R are the expected (co)variances of the random effects and the residuals respectively (Hadfield 2010; Hadfield & Nakagawa 2010). G and R are unknown, and must be estimated from the data by assuming they are structured in a way that can be parametrized by few parameters, as it has been exemplified below for the G case:

$$G = \begin{bmatrix} V_{G_1} \otimes A_{G_1} & 0 \\ 0 & V_{G_2} \otimes A_{G_2} \end{bmatrix} \quad (3)$$

Were the (co)variance matrices (V) are matrices with one parameter to be estimated per response

variable and the structured matrices (A) refer to the phylogenetic structure (A_{G1}) and genus contingency (A_{G2}). The Kronecker product ($\otimes$) allows for possible dependence between random effects (Hadfield 2010; Hadfield & Nakagawa 2010).

In multi-response models, the (co)variance matrix of the previous equation is reformulated including the covariance estimates in the off-diagonal and the respective variances in the diagonal as follows:

$$V_{G1} = \begin{bmatrix} \sigma^2_{u_1} & \sigma_{u_1,u_2} \\ \sigma_{u_2,u_1} & \sigma^2_{u_2} \end{bmatrix} \quad (4)$$

Where σ^2_{u1} is the variance for the first response variable (V_1) and σ^2_{u2} the variance for the second response variable (V_2), while $\sigma_{u1,u2}$ and $\sigma_{u2,u1}$ are the same covariance estimate (C).

Phylogenetic indexes calculation

The phylogenetic signal or phylogenetic heritability it is calculated as follows (Villemereuil & Nakagawa 2014):

$$\lambda = \frac{\sigma^2_p}{\sigma^2_p + \sigma^2_g + \sigma^2_e} \quad (5)$$

Where σ^2_P is the variance of the phylogenetic effect (V_{G1}), σ^2_g is the variance of the cross-genus effect (V_{G2}) and σ^2_e is the residual error (Villemereuil & Nakagawa 2014). Cross-genera variance (i.e. non-phylogenetic variation among genera or genus lability) has been calculated as follows:

$$\gamma = \frac{\sigma^2_g}{\sigma^2_p + \sigma^2_g + \sigma^2_e} \quad (6)$$

And finally, intra-genus variability including measurement error has been calculated as follows:

$$\rho = \frac{\sigma^2_e}{\sigma^2_p + \sigma^2_g + \sigma^2_e} \quad (7)$$

Note also that $\gamma + \rho + \lambda = 1$ (Housworth *et al.* 2004). The three indexes were calculated for the

whole Markov chain random effects and residual samples (once burned and thinned), so the output is a statistical distribution from which the mean and 95% credible intervals can be calculated.

Phylogenetic covariation calculation

From the phylogenetic variances and covariance in equation 4, the evolutionary correlation between response variables can be calculated as follows (Villemereuil 2012):

$$r_{ev} = \frac{\sigma_{u_2,u_1}}{\sqrt{\sigma^2_{u_1} \cdot \sigma^2_{u_2}}} \quad (8)$$

Model specifications

"MCMCglmm" implements a Bayesian approach, estimating the posterior distribution of parameters, from which 95% credible intervals can be obtained (Hadfield 2010). We set independent normal prior distributions for fixed effects and non-informative Inverse-Gamma prior distributions for random effects and residual variances (Villemereuil & Nakagawa 2014). Less informative expanded priors were also used, and highly similar results were obtained.

Uni-response models random effects variance priors were set as V = 1, nu = 0.002. For bi-response models, the random effects variances priors were set as V = diag(2)/2, nu = 2. To achieve convergence, each model was run for 8,000,000 iterations with a 1,000,000 burn-in and a thinning interval of 4,000, reaching an effective sample size between 1,000 and 2,000 in all estimated parameters. When models did not converge, we increased the number of iterations until convergence were achieved. Thinning intervals and the final number of iterations were progressively increased until autocorrelations between samples were found to be <0.1. Convergence of all models was assessed by plots of chain mixing and by the Heidenberg stationary test as a diagnostic. All reported models had a low degree of autocorrelation between iterations and passed the convergence diagnostic, both for fixed and random effects (i.e., the sampled chains

were stationary).

Literature cited

Hadfield, J.D. (2010). MCMCglmm for R. *J. Stat. Softw.*, 33.

Hadfield, J.D. & Nakagawa, S. (2010). General quantitative genetic methods for comparative biology: Phylogenies, taxonomies and multi-trait models for continuous and categorical characters. *J. Evol. Biol.*, 23, 494–508.

Housworth, E.A., Martins, E.P. & Lynch, M. (2004). The Phylogenetic Mixed Model. *Am. Nat.*, 163, 84–96.

Villemereuil, P. (2012). How to use the MCMCglmm R package.

Villemereuil, P. & Nakagawa, S. (2014). General Quantitative Genetic Methods for Comparative Biology. In: (*Modern Phylogenetic Comparative Methods and Their Application in Evolutionary Biology: Concepts and Practice*), {[Garamszegi, L.Z.]}. Springer, New York, USA. 287-303.

Appendix S2. Species-level phylogenetic analyses.

Species-level phylogeny was obtained by pruning the phylogenetic tree reported by Smith & Brown (2018) available in the R package "v.PhyloMaker" (Jin & Qian 2019) by using the "ape" R package (Paradis & Schliep 2018) only keeping species with hydraulic data available in each case, obtaining the same number of observations compared to the genus-level analyses. Some bi-response models implemented using the genus-level phylogeny where also conducted using the species-level phylogeny. As we had only one value per specie, no extra random effect was included, so variance partition was reduced to phylogenetic signal calculation.

Phylogenetic signal results

Variance partitioning for the six hydraulic traits and three environmental principal components related to water availability (PC1), energy input (PC2) and soil depth (PC3). Legend: N: number of species used in each case (for which both phylogenetic and hydraulic data were available), phylogenetic variance (phylogenetic signal, λ) and non-phylogenetic intraspecific variance plus measurement error (ρ). Mean and lower and upper 95% credible intervals (HDP) are shown for each component.

variable	N	λ	λ lower HPD	λ upper HPD	ρ	ρ lower HDP	ρ Upper HDP
HSM	195	0.456	0.228	0.680	0.544	0.320	0.772
Log(Hv)	842	0.654	0.539	0.774	0.346	0.226	0.461
Log(K_l)	616	0.610	0.456	0.753	0.390	0.247	0.544
Log(K_s)	763	0.681	0.569	0.792	0.319	0.208	0.431
Log($\lvert\psi_{min}\rvert$)	358	0.876	0.799	0.940	0.124	0.060	0.201
log_negP50	693	0.709	0.594	0.817	0.291	0.183	0.406
PC1	1329	0.963	0.951	0.975	0.037	0.025	0.049
PC2	1329	0.845	0.796	0.889	0.155	0.111	0.204
PC3	1329	0.907	0.882	0.934	0.093	0.066	0.118

Evolutionary correlations results

Mean of the evolutionary correlation (Cor), credible interval (lower and upper HDP) and p-value reported by bi-response models. Statistically significant evolutionary correlations are highlighted in bold and marginally significant in italics. In the fixed structure column, variables to the right of the "~" symbol are response variables, those to the left are predictors. Abbreviations: "env"(1): individual environmental principal component; env(3): three main environmental principal components; trait: individual hydraulic trait; Affiliation: major evolutionary affiliation (angiosperm or gymnosperm).

Fixed structure	Var. 1	Var. 2	Cor	Lower HDP	Upper HDP	p-value
trait, trait ~ 1 + env(3) * Affiliation	log(Hv)	log(|ψ_{min}|)	0.134	-0.365	0.695	0.641
trait, trait ~ 1	**log(Hv)**	**log(|ψ_{min}|)**	**0.607**	**0.261**	**0.915**	**0.014**
trait, env(1) ~ 1	**log(Hv)**	**PC1**	**-0.807**	**-0.908**	**-0.699**	**0.000**
trait, env(1) ~ 1 + Affiliation	**log(Hv)**	**PC1**	**-0.816**	**-0.922**	**-0.714**	**0.000**
trait, env(1) ~ 1	log(Hv)	PC2	-0.090	-0.334	0.191	0.495
trait, env(1) ~ 1 + Affiliation	log(Hv)	PC2	-0.092	-0.376	0.164	0.501
trait, env(1) ~ 1 + Affiliation	**log(Hv)**	**PC3**	**-0.492**	**-0.689**	**-0.304**	**0.000**
trait, env(1) ~ 1	**log(Hv)**	**PC3**	**-0.493**	**-0.691**	**-0.304**	**0.000**
trait, trait ~ 1 + env(3) * Affiliation	**log(K_s)**	**log(Hv)**	**-0.630**	**-0.851**	**-0.359**	**0.000**
trait, trait ~ 1	**log(K_s)**	**log(Hv)**	**-0.589**	**-0.815**	**-0.348**	**0.000**
trait, trait ~ -1 + env(3) * Affiliation	log(K_s)	log(|ψ_{min}|)	-0.217	-0.663	0.226	0.349
trait, trait ~ 1	*log(K_s)*	*log(|ψ_{min}|)*	*-0.366*	*-0.703*	*0.012*	*0.090*
trait, trait ~ -1 + env(3) * Affiliation	log(K_s)	log(|P50|)	-0.236	-0.579	0.172	0.223
trait, trait ~ 1	**log(K_s)**	**log(|P50|)**	**-0.420**	**-0.674**	**-0.104**	**0.015**
trait, env(1) ~ 1	**log(K_s)**	**PC1**	**0.225**	**0.000**	**0.421**	**0.043**
trait, env(1) ~ 1 + Affiliation	*log(K_s)*	*PC1*	*0.225*	*0.006*	*0.452*	*0.067*
trait, env(1) ~ 1 + Affiliation	log(K_s)	PC2	-0.185	-0.434	0.065	0.160
trait, env(1) ~ 1	log(K_s)	PC2	-0.196	-0.439	0.092	0.155
trait, env(1) ~ 1 + Affiliation	log(K_s)	PC3	0.106	-0.132	0.350	0.395
trait, env(1) ~ 1	log(K_s)	PC3	0.105	-0.147	0.338	0.423
trait, env(1) ~ 1 + Affiliation	**log(|ψ_{min}|)**	**PC1**	**-0.734**	**-0.861**	**-0.599**	**0.000**
trait, env(1) ~ 1	**log(|ψ_{min}|)**	**PC1**	**-0.743**	**-0.868**	**-0.590**	**0.000**
trait, env(1) ~ 1 + Affiliation	log(|ψ_{min}|)	PC2	-0.266	-0.573	0.041	0.127
trait, env(1) ~ 1	log(|ψ_{min}|)	PC2	-0.254	-0.567	0.040	0.118
trait, env(1) ~ 1 + Affiliation	log(|ψ_{min}|)	PC3	0.215	-0.032	0.462	0.101

trait, env(1) ~ 1	*log(|ψ$_{min}$|)*	*PC3*	*0.223*	*-0.032*	*0.453*	*0.097*
trait, trait ~ -1 + env * Affiliation	log(|P50|)	log(Hv)	0.211	-0.256	0.663	0.429
trait, trait ~ 1	**log(|P50|)**	**log(Hv)**	**0.622**	**0.370**	**0.839**	**0.001**
trait, trait ~ -1 + env(3) * Affiliation	**log(|P50|)**	**log(|ψ$_{min}$|)**	**0.773**	**0.582**	**0.926**	**0.000**
trait, env(1) ~ 1	**log(|P50|)**	**log(|ψ$_{min}$|)**	**0.794**	**0.636**	**0.923**	**0.000**
trait, env(1) ~ 1 + Affiliation	**log(|P50|)**	**PC1**	**-0.466**	**-0.658**	**-0.254**	**0.000**
trait, env(1) ~ 1	**log(|P50|)**	**PC1**	**-0.465**	**-0.661**	**-0.257**	**0.000**
trait, env(1) ~ 1 + Affiliation	log(|P50|)	PC2	0.022	-0.250	0.305	0.902
trait, env(1) ~ 1	log(|P50|)	PC2	0.032	-0.225	0.343	0.837
trait, env(1) ~ 1 + Affiliation	log(|P50|)	PC3	-0.147	-0.417	0.102	0.262
trait, env(1) ~ 1	log(|P50|)	PC3	-0.144	-0.390	0.118	0.279

Literature cited

Jin, Y., & Qian, H. (2019). V.PhyloMaker: an R package that can generate very large phylogenies for vascular plants. *Ecography*, 42(8), 1353–1359.

Paradis, E., & Schliep, K. (2018). ape 5.0: an environment for modern phylogenetics and evolutionary analyses in R. *Bioinformatics* 35: 526-528.

Smith, S. A., & Brown, J. W. (2018). Constructing a broadly inclusive seed plant phylogeny. *Am. J. Bot.*, 105(3), 302–314.

878 **Appendix S3. Evolutionary correlations reported by genus-level phylogenetic models using**
879 **observations available for the species-level phylogeny and evolutionary correlations**
880 **reported by species-level phylogeny pruned at the genus level.**

881 For bivariate models including two traits as response variable, only models without fixed effects
882 and models including the three environmental components and its interaction with major
883 evolutionary affiliation (angiosperm or gymnosperm) were implemented.

884 Significant evolutionary correlations (i.e., when the credible interval for the estimated correlation
885 do not include zero) reported by models using a genus-level phylogeny including only observations
886 available for the species-level phylogenetic analyses to check for effects of the different species
887 coverage between phylogenies. Mean of the evolutionary correlation (Cor), credible interval
888 (lower and upper HDP) and p-value reported by bi-response models. In the fixed structure column,
889 variables to the right of the "~" symbol are response variables, those to the left are predictors.
890 Abbreviations: "env"(1): individual environmental principal component; env(3): three main
891 environmental principal components; trait: individual hydraulic trait; Affiliation: major
892 evolutionary affiliation (angiosperm or gymnosperm).

Fixed structure	var1	var2	Cor	Lower HDP	Upper HDP	p-value
trait, env(1) ~ 1 + Affiliation	log(Hv)	PC1	-0.779	-0.926	-0.634	0.000
trait, env(1) ~ 1	log(Hv)	PC1	-0.787	-0.921	-0.647	0.000
trait, env(1) ~ 1 + Affiliation	log(Hv)	PC3	-0.499	-0.749	-0.250	0.001
trait, env(1) ~ 1	log(Hv)	PC3	-0.510	-0.749	-0.260	0.001
trait, trait ~ 1	log(K_s)	log(Hv)	-0.501	-0.850	-0.101	0.049
trait, trait ~ 1 + env(3) * Affiliation	log(K_s)	log(Hv)	-0.603	-0.861	-0.297	0.003
trait, trait ~ 1	log(K_s)	log(|P50|)	-0.394	-0.709	-0.022	0.054
trait, env(1) ~ 1 + Affiliation	log(K_s)	PC2	-0.316	-0.602	-0.011	0.049
trait, env(1) ~ 1	log(K_s)	PC2	-0.341	-0.618	-0.056	0.024
trait, env(1) ~ 1 + Affiliation	log(K_s)	PC3	0.350	0.045	0.633	0.031
trait, env(1) ~ 1	log(K_s)	PC3	0.355	0.065	0.651	0.021
trait, env(1) ~ 1 + Affiliation	log($\|\psi_{min}\|$)	PC1	-0.779	-0.926	-0.623	0.000

trait, env(1) ~ 1	log(|ψ_{min}|)	PC1	-0.783	-0.928	-0.621	0.000
trait, trait ~1	log(|P50|)	log(Hv)	0.495	0.126	0.816	0.014
trait, trait ~ 1	log(|P50|)	log(|ψ_{min}|)	0.485	0.065	0.836	0.054
trait, trait ~ 1 +env(3) * Affiliation	log(|P50|)	log(|ψ_{min}|)	0.598	0.233	0.888	0.008
trait, env(1) ~ 1 + Affiliation	log(|P50|)	PC1	-0.628	-0.863	-0.394	0.000
trait, env(1) ~ 1	log(|P50|)	PC1	-0.618	-0.831	-0.374	0.001

Significant evolutionary correlations (i.e., when the credible interval for the estimated correlation do not include zero) reported by models using a species-level phylogeny pruned at genus-level to check for effects of differences in the topology between phylogenies. Mean of the evolutionary correlation (Cor), credible interval (lower and upper HDP) and p-value reported by bi-response models. In the fixed structure column, variables to the right of the "~" symbol are response variables, those to the left are predictors. Abbreviations: "env"(1): individual environmental principal component; env(3): three main environmental principal components; trait: individual hydraulic trait; Affiliation: major evolutionary affiliation (angiosperm or gymnosperm).

Fixed structure	var1	var2	Cor	Lower HDP	Upper HDP	p-value
trait, env(1) ~ 1 + Affiliation	log(Hv)	PC1	-0.817	-0.924	-0.685	0.000
trait, env(1) ~ 1	log(Hv)	PC1	-0.824	-0.936	-0.696	0.000
trait, env(1) ~ 1 + Affiliation	log(Hv)	PC3	-0.439	-0.705	-0.158	0.008
trait, env(1) ~ 1	log(Hv)	PC3	-0.451	-0.711	-0.159	0.012
trait, trait ~ 1	log(K_s)	log(Hv)	-0.535	-0.844	-0.178	0.018
trait, trait ~ 1 + env(3) * Affiliation	log(K_s)	log(Hv)	-0.626	-0.877	-0.330	0.002
trait, trait ~ 1	log(K_s)	log(|P50|)	-0.398	-0.749	-0.016	0.069
trait, env(1) ~ 1 + Affiliation	log(K_s)	PC2	-0.326	-0.626	-0.013	0.046
trait, env(1) ~ 1	log(K_s)	PC2	-0.332	-0.688	-0.037	0.068
trait, env(1) ~ 1	log(K_s)	PC3	0.334	0.005	0.647	0.045
trait, env(1) ~ 1 + Affiliation	log(|ψ_{min}|)	PC1	-0.774	-0.924	-0.614	0.000
trait, env(1) ~ 1	log(|ψ_{min}|)	PC1	-0.783	-0.933	-0.619	0.000
trait, trait ~1	log(|P50|)	log(Hv)	0.505	0.131	0.814	0.024
trait, trait ~ 1	log(|P50|)	log(|ψ_{min}|)	0.493	0.066	0.858	0.054
trait, trait ~ 1 +env(3) * Affiliation	log(|P50|)	log(|ψ_{min}|)	0.591	0.177	0.906	0.034
trait, env(1) ~ 1 + Affiliation	log(|P50|)	PC1	-0.609	-0.856	-0.349	0.001
trait, env(1) ~ 1	log(|P50|)	PC1	-0.595	-0.831	-0.342	0.001